KP-TR-014-NP

Kairos Power

Kairos Power LLC
707 W. Tower Ave
Alameda, CA 94501

Graphite Material Qualification for the Kairos Power Fluoride Salt-Cooled High-Temperature Reactor

Topical Report

Revision No. 4
Document Date: September 2022

Non-Proprietary

Rev	Description of Change	Date
0	Initial Issuance	December 2020
1	Updates to Chapters 1, 3, 4, 5, and 7. - Chapter 1: Modified discussion of the cover gas system. - Chapter 3: Clarified use of historic data in qualification. - Chapter 4: Clarified qualification plan approach for non-power and power reactor classes. Clarified the methods to address basic properties using data from other grades of graphite pre-turnaround. - Chapter 5: Added further discussion of oxidation including additional testing. Added discussion of testing for infiltration of Flibe. - Chapter 7: Added limitation to qualification plan related to intermediate salt infiltration into the primary. Removed previous Appendix A, Reliability and Integrity Management, and renumbered appendices Added new Appendix B ETU Demonstration of Historical Data Applicability Added new Appendix C Parameter Estimation and Uncertainty Assessment	June 2021
2	Updates to Chapters 1, 2, 3, 4, 5, and 7. - Chapter 1: Clarified the scope of the qualification plan. - Chapter 2: Clarified that Kairos Power intends to qualify ET-10 with conforming changes throughout. - Chapter 3: Clarified the unirradiated graphite testing plan. Added a discussion of fracture toughness and fatigue parameters. Clarified discussion of local property variation and lot-to-lot variation. Expanded the discussion of the purity of ET-10 and added a section to describe the method for determining the unirradiated graphite product specification. - Chapter 4: Added discussion of the standards ORNL used to gather irradiation properties data. Added justifications for measuring irradiated strength and irradiation creep in one direction. Added justification for the irradiation creep test matrix. Added a definition of primary creep rate. Further clarified the method for determining the qualification envelop for irradiated properties. - Chapter 5: Added further discussion of the thermal and pressure gradients in the vessel as they relate to Flibe infiltration. Added discussion of characterization to confirm no significant degradation occurs to ET-10 in Flibe due to chemical compatibility factors. Added discussions of chromium carbide films, abrasion, and erosion. Added	May 2022

	discussion of testing that will be conducted related to oxidation of ET-10 Chapter 7: Added limitations to conform with the changes in the other chapters. Added example calculation to Appendix C Parameter Estimation and Uncertainty Assessment	
3	Changed the method described in Appendix C for the treatment of temperature uncertainty in the irradiation data. Removed References 65 and 66, which are no longer cited in the report.	July 2022
4	Added a test for confirmation of no significant oxidation below the free surface of Flibe to Section 5.3. This is a conforming change to align this report with the response to Request for Additional Information 310 Question 410 (letter KP-NRC-2209-001) regarding the Hermes Preliminary Safety Analysis Report.	September 2022

EXECUTIVE SUMMARY

This topical report describes the qualification for structural graphite used in the safety-related systems of the Kairos Power Fluoride Salt-Cooled, High Temperature Reactor (KP-FHR). The KP-FHR is an advanced Generation IV nuclear reactor being developed for U.S. commercial power generation. The reactor operates near atmospheric pressure and utilizes high temperature fuel and molten salt coolants to provide a high degree of passive safety. The KP-FHR marries this advanced nuclear technology with conventional steam-based electrical power generation.

This document describes the testing required to qualify the structural graphite materials used in the safety-related components of the KP-FHR. This report does not describe testing or modeling for non-safety-related uses of structural graphite. Specifically, the document describes work to apply the existing American Society of Mechanical Engineers (ASME) qualification process for structural graphite materials and to demonstrate environmental compatibility of structural graphite materials for use in safety-related components of the KP-FHR.

Kairos Power is requesting Nuclear Regulatory Commission review and approval of the qualification described in this report for structural graphite materials used for safety-related high temperature components of the KP-FHR for use by licensing applicants under 10 CFR 50 or 10 CFR 52.

Table of Contents

LIST OF ABBREVIATIONS

Acronym	Definition
AG	Against-the-grain
ASME	American Society of Mechanical Engineers
ASTM	American Society for Testing and Materials
BPVC	Boiler and Pressure Vessel Code
CFR	Code of Federal Regulations
CTE	Coefficient of thermal expansion
DOE	Department of Energy
EBC	Equivalent boron content
FHR	Fluoride Salt-Cooled High Temperature Reactor
FSAR	Final Safety Analysis Report
GDMS	Glow Discharge Mass Spectrometry
INL	Idaho National Laboratory
ISI	In-service inspection
KP-FHR	Kairos Power Fluoride Salt-Cooled, High Temperature Reactor
LWA	Limited Work Authorization
LWR	Light Water Reactor
MANDE	Monitoring and Non-Destructive Examination
MHTGR	Modular High Temperature Gas Reactor
MSRE	Molten Salt Reactor Experiment
NRC	Nuclear Regulatory Commission
ORNL	Oak Ridge National Laboratory
PDC	Principal Design Criteria
PIRT	Phenomena Identification and Ranking Table
PSAR	Preliminary Safety Analysis Report
RG	Regulatory Guide
TC	Thermal conductivity
TRISO	Tri-Structural Isotropic
WG	With-the-grain

1 INTRODUCTION

Kairos Power LLC (Kairos Power) is pursuing the design, licensing, and deployment of reactors based on a Fluoride Salt-Cooled, High Temperature Reactor (KP-FHR) technology. The first demonstration of this technology will be a non-power reactor referred to as Hermes, followed by a power reactor referred to as KP-X. License applications for these reactors will rely on the use of qualified structural graphite materials in select safety-related applications. The structural graphite materials qualification program relies on both materials testing and modeling to ensure the performance of the safety-related structural graphite materials. This report details the methodology for safety-related structural graphite materials qualification for the KP-FHR. The methodology is generally consistent with Section III, Division 5, ASME Boiler and Pressure Vessel Code (BPVC), "Rules for Construction of Nuclear Power Plant Components, High Temperature Reactors," (hereinafter referred to as the "Division 5 code" or "code,") requirements (Reference 1). The actual code year used in the design will be specified in supporting licensing applications and permits.

The Division 5 code (2017 edition) does not specifically list any structural graphite material as already qualified for use in a nuclear power reactor. Instead, the code provides steps to qualify a grade of graphite. The code also requires the user to address oxidation and irradiation effects of the structural materials. Although the code does not directly address compatibility with molten salts, Kairos Power has considered that interaction in this qualification plan. Kairos Power also conducted an evaluation of phenomena to identify significant degradation phenomena and to develop the testing and modeling qualification presented in this report.

The qualification plan described in this report addresses material qualification methods for a power reactor KP-FHR and a non-power KP-FHR, Hermes. NRC requirements and guidance differs for power and non-power reactors with respect to quality assurance programs. Kairos Power is implementing the quality assurance requirements of the Division 5 code for the power reactor application. The quality assurance program will be applied to data relied on to demonstrate that the structural graphite material can perform its safety function as described in this qualification plan (see Section 1.2).

For the Hermes reactor application, Kairos Power is implementing a quality assurance program based on ANSI/ANS-15.8-1995, "Quality Assurance Program Requirements for Research Reactors," (ANSI/ANS-15.8), which is endorsed by NRC Regulatory Guide 2.5, "Quality Assurance Program Requirements for Research and Test Reactors." For this reason, Kairos Power is departing from the Division 5 code requirements that would require an NQA-1 based quality assurance program, including HAB-3125, HAB-3127, and HHA-III-2000, in the generation of testing data to support a non-power reactor design and licensing application.

This report describes a three-part structural graphite qualification plan: qualification of unirradiated graphite, qualification of irradiated graphite, and qualification of graphite in Flibe, a molten salt made from a mixture of lithium fluoride (LiF) and beryllium fluoride (BeF2). Seismic qualification of structural graphite components is outside the scope of this report (See Section 6 for more information).

Inspection and aging management considerations for the KP-FHR will be described as part of the licensing application of the KP-FHR. Kairos Power does not seek approval for the nuclear component life management program elements as part of this report.

Kairos Power seeks NRC review and approval for the qualification plan described in this report for safety-related structural graphite materials in a KP-FHR for use by licensing applicants under 10 CFR 50 or 10 CFR 52.

1.1 DESIGN OF THE KP-FHR

To facilitate NRC review and approval of this report, design features considered essential to the KP-FHR technology are provided in this section. These key features are not expected to change during the ongoing detailed design work by Kairos Power and provide the basis to support the safety review. Should fundamental changes occur to these design features or revised regulations be promulgated that affect the conclusions in this report, such changes will be reconciled and addressed in future license application submittals.

1.1.1 Design Background

In the last decade, U.S. National laboratories and universities have developed pre-conceptual Fluoride-Cooled High-Temperature Reactor (FHR) designs with different fuel geometries, core configurations, heat transport system configurations, power cycles, and power levels. More recently, the University of California at Berkeley developed the Mark 1 pebble-bed FHR, incorporating lessons learned from the previous decade of FHR pre-conceptual designs. (Reference 2). Kairos Power has built on the foundation laid by the U.S. Department of Energy (DOE) sponsored, university Integrated Research Projects to develop the KP-FHR. Although not intended to support the findings necessary to approve this report, additional design description information is provided in the "Design Overview of the Kairos Power Fluoride Salt-Cooled, High Temperature Reactor" Technical Report (Reference 3).

1.1.2 Classes of KP-FHR Reactors

Kairos Power is developing both a non-power reactor KP-FHR and a power reactor KP-FHR. The operating parameters discussed in this topical report will apply to both reactor classes. The non-power reactor KP-FHR will operate at lower power level and temperature than the power reactor. Table 1 contains key parameters for the power reactor KP-FHR.

One difference that will have a bearing on data needed to qualify structural graphite is the expected lifetime of the component in the reactor. The non-power reactor reflector lifetime is anticipated to be consistent with the operating life of the reactor (5 years, 1 year commissioning + 4 years operation), while the reflector lifetime in the power reactor is anticipated to be on the order of [[ ]] .

1.1.3 Key Features

The KP-FHR technology integrates key design features and material choices into a physically compact, intrinsically safe, high temperature reactor which will be built with existing, industrially proven materials. Key design features of the KP-FHR include the use of high temperature fuel, high boiling point molten salt coolants, and low-pressure operation. This combination of the Tri-Structural Isotropic (TRISO) particle fuel, stable high boiling temperature fluoride salt coolant, and low operating stresses results in a robust reactor design with intrinsic passive safety.

The fuel in the KP-FHR is based on the TRISO high-temperature fuel. TRISO fuel is a carbon matrix coated particle fuel, originally developed for high-temperature gas-cooled reactors, in a pebble fuel element. Coatings on the particle fuel provide retention of fission products to temperatures approaching 1600°C. The primary coolant that is used in safety-related systems is a mixture of lithium fluoride (LiF) and beryllium fluoride (BeF_2) salts in a ratio of approximately 2:1. This F-Li-Be based salt, i.e., 'Flibe' has been proven as an effective nuclear coolant in the Molten Salt Reactor Experiment (MSRE) program and the operation of the MSRE nuclear reactor. Furthermore, there has been significant research into the stability and compatibility of Flibe in nuclear applications since the operation of the MSRE. The KP-FHR is a low-pressure reactor which operates with a modest overpressure in the reactor vessel head space to minimize contamination of the primary coolant and oxidation in the primary system. For the power reactor, the overpressure also ensures that [[

]] .

1.1.3.1 Heat Transport Systems

A power reactor KP-FHR will include at least two heat transfer loops. A primary loop contains Flibe and maintains cooling in the core. Other heat transfer loop(s) remove heat from the primary system during normal operations. Figure 1 shows three heat transport loops for the power reactor KP-FHR and the operating temperature range (550-650°C). A non-power KP-FHR will include one heat transfer loop that transfers heat to air (see Figure 1). The non-power reactor hot leg will operate up to 650°C and the cold leg returns the Flibe to the reactor vessel at 550°C. The test reactor does not include a power conversion loop.

The design includes decay heat removal for both normal and postulated event conditions. Normal decay heat removal functions follow normal shutdowns and postulated events. The design also includes a passive decay heat removal function, which along with natural circulation in the reactor vessel, is used to remove decay heat in response to a postulated event. This system does not rely on electrical power to achieve and maintain safe shutdown for postulated events.

1.1.3.2 Cover Gas System

A cover gas is provided to maintain an atmosphere of inert gas over the Flibe free surface in the reactor. This cover gas removes tritium, oxygen, and other gases or particulates for further treatment. In addition, the cover gas assists in Flibe level control during operation and maintenance and purge gas flows to prevent Flibe vapor and aerosols from entering into cold parts of reactor head components. Reactor cover gas aids in maintaining a non-corrosive environment in concert with the other reactor coolant chemistry controls. This cover gas system maintains an inert environment in the head space of the reactor vessel so that no more than trace levels of oxygen are present in the reactor vessel during normal operation and planned transients. See Section 5.2 for further information about how oxidation is considered in the qualification of the structural graphite.

1.1.3.3 Containment Approach

The KP-FHR technology uses a functional containment approach, like the Modular High Temperature Gas-Cooled Reactor (MHTGR) rather than the low-leakage, pressure-retaining containment structure that is typically used for light water reactors (LWRs). The KP-FHR functional containment safety design objective is designed to meet 10 CFR 50.34 (10 CFR 52.79) offsite dose requirements at the plant's exclusion area boundary with margin. A functional containment is defined in Regulatory Guide (RG) 1.232, "Guidance for Developing Principal Design Criteria for Non-Light Water Reactors" as a "barrier, or set of barriers taken together, that effectively limit the physical transport and release of radionuclides to the environment across a full range of normal operating conditions and postulated event conditions. RG 1.232 includes an example design criterion for the functional containment (MHTGR Criterion 16). As also stated in RG 1.232, the NRC has reviewed the functional containment concept and found it "generally acceptable," provided that "appropriate performance requirements and criteria" are developed. The NRC staff has developed a proposed methodology for establishing functional containment performance criteria for non-LWRs, which is presented in SECY-18-0096, "Functional Containment Performance Criteria for Non-Light-Water-Reactors." This SECY document has been approved by the Commission.

The functional containment approach for the KP-FHR is to control radionuclides primarily at their source within the coated fuel particle under normal operations and postulated event conditions without requiring active design features or operator actions. The KP-FHR design relies primarily on the multiple barriers within the TRISO fuel particles and fuel pebble to ensure that the dose at the site boundary (from postulated events) meets regulatory limits. Additionally, in the KP-FHR (but not in MHTGR designs), the molten salt coolant serves as an additional barrier providing retention of fission products that could escape the fuel particle and fuel pebble barriers. This additional retention barrier is a key feature of the enhanced safety and reduced source term in the KP-FHR.

1.1.3.4 Graphite Reflector Assembly

The KP-FHR includes a reflector assembly which is made of graphite. The reflector assembly provides thermal inertia and moderation for the neutrons and shields the outer metallic structures from fast neutrons while reflecting the neutrons back into the active core region. The graphite reflector is positively buoyant in Flibe.

The *Design Overview of the Kairos Power Fluoride Salt-Cooled, High Temperature Reactor* Technical Report (KP-TR-001, Reference 3) contains further information about the design of the graphite reflector. The primary safety functions of the graphite reflector assembly are to ensure coolant flow paths through the reactor vessel during normal and off-normal conditions and to provide for the insertion of negative reactivity through control elements.

[[

]] . The *Metallic Materials Qualification for the Kairos Power Fluoride Salt-Cooled High Temperature Reactor* Topical Report (KP-TR-013, Reference 4) discusses the qualification of metallic materials in the KP-FHR in the reactor core.

1.2 REGULATORY INFORMATION

The KP-FHR is anticipated to be licensed under Title 10 of the Code of Federal Regulations (10 CFR) using a licensing pathway provided in Part 50 or Part 52. Applicants for construction permits for facilities licensed under 10 CFR 50 are required to provide a Preliminary Safety Analysis Report (PSAR), which provides a safety assessment of the facility in accordance with 10 CFR 50.34(a). Applicants for a Limited Work authorization (LWA) for a power reactor are required to submit a safety analysis that meets 10 CFR 50.34 for the scope of the LWA per 10 CFR 50.10(d)(3)(i). Subsections within 10 CFR 50.34(a) relevant to the requirement to describe design characteristics of the KP-FHR structural graphite materials are listed below (note these are required to be updated as part of the operating license application in the Final Safety Evaluation Report (FSAR) per 10 CFR 50.34(b)(4)):

> *50.34(a)(1)(ii)(B) The extent to which generally accepted engineering standards are applied to the design of the reactor.*
>
> *50.34(a)(1)(ii)(C) The extent to which the reactor incorporates unique, unusual or enhanced safety features having a significant bearing on the probability or consequences of accidental release of radioactive materials.*
>
> *50.34(a)(2) A summary description and discussion of the facility, with special attention to design and operating characteristics, unusual or novel design features, and principal safety considerations.*
>
> *50.34(a)(3)(ii) The preliminary design of the facility including the design bases and the relation of the design bases to the principal design criteria.*

Similarly, applicants for combined licenses for power reactors licensed under 10 CFR 52 are required to provide a FSAR which provides a safety assessment of the facility in accordance with 10 CFR 52.79. Subsections relevant to the design and performance of structural graphite materials are as follows:

> *52.79(a)(2) A description and analysis of the structures, systems, and components of the facility with emphasis upon performance requirements, the bases, with technical justification therefor, upon which these requirements have been established, and the evaluations required to show that safety functions will be accomplished. It is expected that reactors will reflect through their design, construction, and operation an extremely low probability for accidents that could result in the release of significant quantities of radioactive fission products. The descriptions shall be sufficient to permit understanding of the system designs and their relationship to safety evaluations. Items such as the*

reactor core, reactor coolant system, instrumentation and control systems, electrical systems, containment system, other engineered safety features, auxiliary and emergency systems, power conversion systems, radioactive waste handling systems, and fuel handling systems shall be discussed insofar as they are pertinent.

52.79(a)(ii) The extent to which generally accepted engineering standards are applied to the design of the reactor.

52.79(a)(2)(iii) The extent to which the reactor incorporates unique, unusual or enhanced safety features having a significant bearing on the probability or consequences of accidental release of radioactive materials.

52.79(a)(2)(iv) The safety features that are to be engineered into the facility and those barriers that must be breached as a result of an accident before a release of radioactive material to the environment can occur. Special attention must be directed to plant design features intended to mitigate the radiological consequences of accidents.

52.79(a)(4)(ii) The design of the facility including the design bases and the relation of the design bases to the principal design criteria.

Similar requirements to these are also included in 10 CFR 52.47 for Standard Design Certifications; 10 CFR 52.137 for Standard Design Approvals; and 10 CFR 52.157 for manufacturing licenses.

Test reactor applicants that seek a Limited Work Authorization (LWA) are also required to submit a safety analysis that meets 10 CFR 50.34 for the scope of the LWA per 10 CFR 50.10(d)(3)(i). The requirements listed above for power reactors are the same as for test reactor applicants with the exception of 10 CFR 50.34(a)(1)(ii). The portion of 10 CFR 50.34(a) relevant to structural graphite materials in a test reactor in 10 CFR 50.34(a)(1)(i) is:

50.34(a)(1)(i) A description and safety assessment of the site on which the facility is to be located, with appropriate attention to features affecting facility design. Special attention should be directed to the site evaluation factors identified in part 100 of this chapter. The assessment must contain an analysis and evaluation of the major structures, systems and components of the facility which bear significantly on the acceptability of the site under the site evaluation factors identified in part 100 of this chapter, assuming that the facility will be operated at the ultimate power level which is contemplated by the applicant. With respect to operation at the projected initial power level, the applicant is required to submit information prescribed in paragraphs (a)(2) through (a)(8) of this section, as well as the information required by this paragraph, in support of the application for a construction permit, or a design approval.

Facilities licensed under 10 CFR Part 50 are also required to describe Principal Design Criteria (PDC) in their PSAR report supporting a construction permit and operating license application as described in 10 CFR 50.34(a)(3)(i). Likewise, applicants for standard design certifications, combined licenses, standard design approvals, and manufacturing licenses must include the PDC for a facility as described in 10 CFR 52.47(a)(3)(i), 10 CFR 52.79(a)(4)(i), 10 CFR 52.137(a)(3)(i), and 10 CFR 52.157(a). The PDC for the KP-FHR have been established in the Kairos Power Topical Report, "Principal Design Criteria for the Kairos Power Fluoride Salt Cooled High Temperature Reactor" (Reference 5). The specific PDC in this report, which rely on or credit the design and performance of structural graphite materials include PDCs 1, 34, 35, and 74. These PDC are discussed below.

PDC 1 requires that:

Structures, systems, and components which are safety significant shall be designed, fabricated, erected, and tested to quality standards commensurate with the safety significance of the functions to be performed. Where generally recognized codes and standards are used, they shall be identified and evaluated to determine their applicability, adequacy, and sufficiency and shall be supplemented or modified as necessary to assure a quality product in keeping with the required safety function. A quality assurance program shall be established and implemented in order to provide adequate assurance that these structures, systems, and components will satisfactorily perform their safety functions. Appropriate records of the design, fabrication, erection, and testing of structures, systems, and components which are safety significant shall be maintained by or under the control of the nuclear power unit licensee throughout the life of the unit.

PDC 34 requires that:

A system to remove residual heat shall be provided. For normal operations and anticipated operational occurrences, the system safety function shall be to transfer fission product decay heat and other residual heat from the reactor core at a rate such that specified acceptable system radionuclide release design limits and the design conditions of the reactor coolant boundary are not exceeded.

Suitable redundancy in components and features and suitable interconnections, leak detection, and isolation capabilities shall be provided to ensure that the system safety function can be accomplished, assuming a single failure.

PDC 35 requires that:

A system to assure sufficient core cooling during postulated accidents and to remove residual heat following postulated accidents shall be provided. The system safety function shall be to transfer heat from the reactor core during and following postulated accidents such that fuel and reactor internal structure damage that could interfere with continued effective core cooling is prevented.

PDC 74 requires that:

The design of the reactor vessel and reactor system shall be such that their integrity is maintained during postulated accidents (1) to ensure the geometry for passive removal of residual heat from the reactor core to the ultimate heat sink and (2) to permit sufficient insertion of the neutron absorbers to provide for reactor shutdown.

The use of structural graphite materials in Flibe salt environments as a reflector is considered to represent a new and unique feature not typical of existing licensed light water reactor designs. This report provides information relevant to the content expected to be provided in a safety analysis report consistent with the regulations cited above. The safety function of the structural graphite reflector materials is to maintain a physical geometry for the reactor core, support core cooling and heat removal, and provide a pathway for reactivity control elements insertion. The structural graphite materials perform these safety functions by remaining in place. For the material qualification, remaining in place is represented by maintaining its structural integrity during normal operation and postulated events. The qualification plan described in this report will provide the necessary qualification information and data to demonstrate that structural graphite in the reactor core is appropriate for use in a coolant flow path for these safety functions and support conformance, in part, to PDCs 1, 34, 35, and 74. This report does not describe testing or modeling for non-safety-related uses of structural graphite. Analyses for other SSCs in the reactor vessel may

reference graphite properties not covered in this topical report. Those graphite properties are considered out of scope for this report because they do not relate to the safety function of the graphite reflector material.

2 NUCLEAR GRAPHITE AND GRAPHITE SELECTION

Nuclear graphite materials have been used in multiple industrial applications, including conventional nuclear reactors, advanced nuclear reactor experiments, non-nuclear but comparable industrial applications, and molten salt reactors. This section provides background on those industrial applications. This section also discusses the grade of graphite selected for the KP-FHR as well as an overview of the material qualification plan. Finally, this section discusses the process Kairos Power used to identify phenomena of interest to structural graphite material qualification.

2.1 BACKGROUND ON NUCLEAR GRAPHITE

Graphite has been used in nuclear industry for over 70 years. In advanced reactors it is used as a moderator, reflector, and structural component due to its low neutron absorption cross-section, large scattering cross section and thermal and chemical stability.

Synthetic graphite is typically manufactured from filler coke and binder pitch. Coke and pitch are the by-products of petroleum refining and coal coking processes. Nuclear graphite is usually manufactured from isotropic cokes and is processed to be near-isotropic or isotropic materials. Figure 2 shows the major processing steps in the manufacturing of nuclear graphite. The step in which green artifact is formed is a critical processing step that determines the characteristics of the final material. The common forming methods for making graphite include extrusion, molding, iso-static molding and vibrating molding. After baking (carbonization), the artifact is typically impregnated with pitch and re-baked to densify it. The baked stock is then graphitized to convert the material to graphite. Additional halogen purification may be required for high purity product, e.g., some nuclear graphite. Typical graphite processing time is 6 - 9 months.

The forming and densification processes impart property variations within the billet. The properties will be different in the forming direction compared with the direction perpendicular to forming. Moreover, a density gradient will exist from billet edge to center. These variations will be quantified for the selected grades of graphite in the structural graphite material qualification plan, outlined in Section 3.3. In addition, variations in properties will occur from billet to billet within a batch, and between production lots. Typically, in extruded graphite the in-billet variations are significant and can exceed lot-to-lot variations. In iso-statically molded graphite, the in-billet variations are less than those in extruded graphite and will be on the same order as the lot-to-lot variations (Reference 6).

Graphite has some unique characteristics and more property variation compared to metallic materials. For example, the graphite strength increases with the temperature. Meanwhile, the variation of graphite properties mainly comes from the processing method and process control. The processing method generates certain property patterns and results in natural property variations that are not improved by quality control efforts. Iso-static molding produces more uniform material, compared to extrusion and molding. Property gradients can normally be observed from center to periphery and from end to middle of an iso-statically molded billet.

Graphite properties are inherently anisotropic because of the anisotropy in graphite grain structure and orientation. They can be different in the direction parallel to coke grain (With-the-Grain, WG) than in the direction perpendicular to coke grain (Against-the-Grain, AG). As a result, the ratio of anisotropy in the material is an important parameter. Anisotropy ratio is defined as the ratio of the coefficient of thermal expansion (CTE) in the AG direction to the WG direction (i.e., CTE_{AG}/CTE_{WG}). Other properties including strength, thermal conductivity, and electrical resistivity vary in AG and WG directions, but by a different ratio. Although graphite mechanical strength and toughness are responsible for graphite's structural integrity, the CTE and the thermal conductivity are important factors in thermal

stress. The tolerance of graphite to stress is largely associated with its microstructure and porosity. The graphite properties, their characteristics and performance attributes are highlighted in Table 2.

Irradiation causes property changes as a function of irradiation fluence and irradiation temperature. One of the most important changes is irradiation-induced dimensional change. As the irradiation fluence increases, graphite first shrinks (its density increases) until a fluence called the *turnaround*, then expands. The density comes back to its pre-irradiated level at a fluence call the *crossover*, after which the graphite keeps expanding. Turnaround and crossover fluences decrease with increasing irradiation temperature, as shown in Figure 3. Internal stresses induced by irradiation-induced dimensional change are generally much higher than stresses from external constraints. These stresses are partially relieved by irradiation creep but may eventually lead to failure of the graphite directly exposed to the core. The end-of-life fluence is generally considered to be between turnaround and crossover and depends on the flux and temperature profile within the component, the geometry of the component, and the graphite properties, including anisotropy and strength. End-of-life fluence can be estimated with stress analysis of the specific component geometry.

Irradiation also affects mechanical and thermal properties. Some general trends have been observed from numerous past irradiation experiments. The strength loosely corresponds with the dimension change, i.e., it increases in the densification region (before turnaround), then decreases after the turnaround. Modulus has a similar trend. Irradiation creep rate increases with irradiation temperature. CTE only initially increases, then decreases as an overall trend. Above mentioned properties all show strong irradiation temperature dependency. Thermal conductivity degrades more quickly and decreases almost immediately to ~30% of unirradiated values and then levels off. Thermal conductivity also shows less temperature and irradiation dose dependency after it reaches a "saturation limit" (References 7 and 8). In summary, the results of past irradiation experiments show that property change before turnaround can be reasonably predicted; but after the turnaround, the property change is less predictable.

2.2 GRAPHITE SELECTION FOR THE KP-FHR

Kairos Power investigated the global nuclear graphite market to identify a suitable candidate graphite grade and found that the ETU-10 fine grain iso-statically molded graphite from Ibiden best met its needs.

Ibiden is a Japanese global company. The Fine Graphite Material/Machining Business Unit produces graphite products in Japan and Korea. Ibiden's fine grain iso-statically molded graphite products have been well established in the graphite industry. ET-10 is a dual-use product serving semiconductor, electronics and the solar industry. The purified version, designated as ETU-10, can be used in the nuclear industry. The dual use grade graphite is also a more reliable product for long term supply. Although ETU-10 is a newer grade of graphite to the nuclear community, a reasonable amount of irradiation data has been generated through testing at Oak Ridge National Laboratory (ORNL), with the exception of irradiation creep data (Reference 9). The qualification plan in this report will address that need for additional data, as discussed further in Section 4. ET-10 is a pitch coke based superfine grain iso-molded graphite with maximum coke particle size of 40μm. ETU-10 is the halogen gas purified ET-10 (see Chapter 3 for more information). The typical properties for ET-10 and ETU-10 provided by Ibiden are shown in Table 3 and Figure 4 through Figure 7.

In the 1960s, the Molten Salt Reactor Experiment (MSRE) conducted by ORNL used a grade of graphite referred to as CGB grade graphite. CGB grade graphite was able to block the Flibe molten salt (used in MSRE) infiltration due its special pore structure, but the grade is no longer commercially available. In the MSRE experiment the molten salt contained fuel which could potentially generate hot spots in graphite, thereby significantly increasing the local temperature and shortening the graphite service life (Reference 10). Because the KP-FHR's fuel is contained in TRISO

pebbles, the same concern about hot spots due to Flibe infiltration does not exist. Instead, qualification of the graphite in Flibe will focus on verifying minimal change to physical and chemical properties of the material and ensuring that any changes to thermophysical or mechanical properties are properly accounted for.

2.3 EXPERT REVIEW PHENOMENA IDENTIFICATION AND RANKING

The nuclear graphite community has developed significant knowledge of graphite properties and their relationship to material performance over many decades. In December 2001, NRC published *Phenomenon Identification and Ranking Tables (PIRTs) for Loss-of-Coolant Accidents in Pressurized and Boiling Water Reactors Containing High Burnup Fuel*, (NUREG/CR-6944, Vol. 5, Reference 11) which identifies and ranks the phenomena occurring during selected transient and accident scenarios in both pressurized water reactors and boiling water reactors containing high burnup fuel. In 2007, Idaho National Laboratory (INL) issued *Graphite Technology Development Plan* (Reference 12), based on the phenomena identified in NRC NUREG/CR-6944. The INL report proposed the research areas for graphite development to address areas of low knowledge and high importance. Table 4 provides those research areas along with their relationship to the KP-FHR structural graphite material qualification plan. The proposed research areas from the INL report are consistent with the needs for graphite qualification for the KP-FHR, with two differences:

1. Oxidation, identified as a research area in the INL report, is not a concern for the KP-FHR (See Section 5.2)
2. Flibe compatibility with graphite is a phenomenon that was not considered in the INL report since it was based on a gas cooled reactor but will be evaluated in the Kairos Power graphite qualification process.

Two other organizations documented identification of phenomena of interest to a KP-FHR which informed the qualification plan described in this report. First, ORNL identified technical gaps for molten salt reactors in ORNL/SPR-2019/1089 (Reference 13) which looked at phenomena important to MSRs that use dissolved fuel. The ORNL report drew some specific conclusions about gas permeability as a phenomenon for MSRs that use dissolved fuel, that do not apply to a KP-FHR which uses pebble fuel. The ORNL report also discussed a need for additional measurement of material properties under irradiation, in particular shrinking and swelling of the material under fluence. Section 4 discusses how of irradiation effects on material properties is addressed in the structural graphite material qualification plan. Finally, the ORNL report identified infiltration and fluorination as phenomena of interest to graphite in a molten salt environment. Section 5 discusses how environmental compatibility is factored into the structural graphite material qualification plan. Second, Georgia Institute of Technology published a PIRT for material selection and possible material degradation mechanisms in fluoride salt cooled high temperature reactors (Reference 14). The GA Tech PIRT discussed graphite in the context of tritium control and corrosion control which are out of scope of this report and did not identify concerns about the interaction between molten salt and graphite.

2.4 QUALIFICATION PLAN OVERVIEW

As noted in Section 1.1.3.4, the reflector assembly is made of graphite which will be exposed to a neutron fluence and a Flibe coolant environment. The qualification approach for structural graphite to be used in a KP-FHR include three basic elements: 1) confirmation of the unirradiated graphite mechanical and thermal properties used in the design of the structural graphite for the material to perform its safety function, 2) confirmation that the graphite will maintain its structural integrity within a neutron flux; and 3) confirmation that the grade is compatible with a Flibe coolant environment. These elements are described in Sections 3, 4, and 5 respectively, of this report.

3 QUALIFICATION OF UNIRRADIATED GRAPHITE MECHANICAL AND THERMAL PROPERTIES

The Division 5 code provides a process to qualify graphite materials for use in a high temperature nuclear power reactor. This process is generally applied to the structural graphite for a KP-FHR, with one exception for unirradiated graphite discussed in Section 3.1 and another exception for irradiated graphite discussed in Section 4.3. The Division 5 code provides requirements and guidance on the qualification of as-manufactured graphite, also referred to as unirradiated graphite in this report. The applicable articles are highlighted in Table 5. The process described in the code provides a method to demonstrate that the selected graphite grade (ET-10) is able to meet the design criteria for a component. This section discusses how Kairos Power will use the Division 5 code qualification process to characterize the properties of unirradiated structural graphite. The mechanical and thermal properties data obtained from the qualification process described in this section will be used to assess the structural integrity of ET-10 using the probabilistic approach described in the Division 5 code, Article HHA-II-3000 and its sub-articles on material reliability curve parameters and design allowable stress values.

Sections 3.1, 3.2 and 3.3 describe the application of the Division 5 code and corresponding ASTM Standards requirements to the measurement of graphite mechanical and thermal properties, the sampling requirements, and the measurement of graphite purity, respectively. The measurements of mechanical and thermal properties also capture the effect of pore size on graphite material properties, so no separate pore size measurements are included in this qualification plan. This approach is also consistent with the Division 5 code.

Ibiden is an ISO-9000 certified facility. All the mechanical and thermal property tests, conducted or to be conducted by Ibiden, described in Section 3 follow this quality standard. In a future license application, Kairos Power will address the acceptability of this data to satisfy the Division 5 code quality standards as discussed in Chapter 1.

ETU-10 is halogen gas purified ET-10. The mechanical and thermal properties remain the same after purification by halogen gas. For example, SGL Carbon designates different purity identifiers to the same grade graphite with different purity levels (Reference 15). Similarly, Ibiden provided Kairos Power with the data in Table 3, which shows that the physical properties for ET-10 and ETU-10 are the same. For more information about the purity specification for ET-10, see Section 3.3. The qualification plan in this document will demonstrate that ET-10 material is qualified for use as the material for the reflector structure to perform its safety function. In the qualification plan, Kairos Power will use ET-10 graphite to qualify the mechanical and thermal properties for the graphite to be used for constructing a KP-FHR.

3.1 MECHANICAL AND THERMAL PROPERTIES

The objective of the testing in this section is to generate the representative data of each property, and to evaluate the intra-billet and billet-to-billet variation of the graphite from 3 graphitization charges. The data will also be used to determine the probability of failure and used as inputs for modeling (not covered in this report).

The qualification plan for structural graphite will meet HHA-II-2000 in that the parameters used in the design necessary for the structural graphite to meet its safety function will be included in the material data sheet (MDS), with the exception of seismic design (See Chapter 6). Tests to collect the property information will be conducted as described in Table 6 for ET-10. Table 6 also indicates the number of specimens, specimen orientation, and test temperatures that will be used for each property test conducted.

Table 7 lists the ASTM standards to be followed in the data generation. Data analysis will follow the method described in Appendix A. Collection of the property data described in this section for the structural graphite material will be

used in both the non-power and power reactor license applications. In the license applications, the mechanical and thermal properties for the structural graphite will be demonstrated to be compliant with the Division 5 code and ASTM testing requirements listed in Table 5.

The Division 5 code specifies requirements for room temperature and high temperature strength testing. However, graphite strength increases with temperature (see Figure 4), therefore, the use of room temperature strength data is conservative for the purpose of material qualification and for use in safety analyses. In addition, a high temperature ASTM standard (method) for strength testing for graphite does not exist. Therefore, Kairos Power will not pursue the use of high temperature strength data for qualification or analysis.

A few explanations about the tests listed in Table 6 are highlighted below:

- Three strength parameters at room temperature will be measured, i.e., flexural, tensile, and compressive strength.
- Bulk density will be measured at room temperature.
- Dynamic Young's modulus and shear modulus will be measured at room temperature.
- CTE and thermal conductivity (TC) tests will use the same specimen for the measurements at all temperatures.
    - The temperature range over which testing for CTE and TC will be conducted will envelope the KP-FHR design basis operation and postulated event conditions, i.e., 25°C to 825°C with increments of 200°C.
- The number of specimens per data set is determined by the sample cutting plan as discussed below.

Based on the Division 5 code, HHA-III-4100, *As-Manufactured Graphite*, the following sampling plan is proposed to determine the number of billets and specimens to use in material property characterization testing listed in Table 6, as well as the sampling locations in the billet.

- [[ ]] billets will be tested with test billets taken from [[ ]] charges, with 4 billets per charge.
- [[ ]] WG and [[ ]] AG specimens will be tested per property per billet. For [[ ]] in AG direction. In each billet, specimens will be taken from [[ ]] positions along the length direction of the billet. [[ ]] specimens in the WG and AG directions from both the [[ ]] of a slice will be taken from the [[ ]] positions, (i.e., [[ ]]). The cutting pattern is illustrated in Figure 8.

The Division 5 code, HHA-III-3100, lists the parameters to be tested in the material data sheet. The article includes fracture toughness in the list of parameters but does not state how the parameter should be used. In metallic materials, fracture toughness is often used in evaluation of damage tolerance for a material. A future license application would address the aspects of the Division 5 code related to damage tolerance for structural graphite, but that is out of the scope of this topical report. Kairos Power does not rely on the fracture toughness parameter to demonstrate the ability to perform its safety function as outlined in this qualification plan. For that reason, Kairos Power is deviating from the Division 5 code by not including fracture toughness in the material data sheet for the purposes of demonstrating material qualification of the reflector to perform its safety function.

3.1.1 Fatigue

The three phenomena to consider related to fatigue of buoyant graphite in Flibe are thermal striping, high cycle fatigue (HCF), and low cycle fatigue (LCF). Flibe's inherent fluid properties (i.e., low thermal conductivity and high

Prandtl number) inhibit fluid to solid convective heat transfer and hence, strongly reduce the risk of thermal striping and HCF, so those phenomena are not considered further in the qualification plan. Thermal transients potentially could lead to cases of low cycle fatigue (LCF). The limited temperature amplitude of thermal transients and the low CTE value of graphite (compared to steel) will translate into non-zero mean stresses (defined as the mathematical average between the two stress extrema) for fatigue loads as well as high (i.e., >> -1) R-ratio values (defined as the ratio of the minimum stress to maximum stress). As a result, Kairos Power anticipates the effects of fatigue on the structural integrity of the graphite reflector blocks to be limited. This applies to both Hermes and KP-X, although Hermes is expected to experience smaller temperature variations. Note that, as stated in Chapter 6, seismic loads are not in the scope of this topical report.

The strength measurement values reported by R.J. Price (REF) for two medium-grained graphite grades (i.e., H-451 and PGX), pre- and post-irradiation reveal that:

- Fatigue strength increases with increasing fast fluences before turnaround
- No Fatigue strength steadily decreases with the number of cycles but the reduction in strength remains limited for low cycle fatigue
- The two graphite grades exhibit comparable behavior when normalized by their tensile strength
- Higher R-ratios (with R = Min Stress / Max Stress) lead to longer fatigue lives.

Given the relationship between the material's cyclic (fatigue) and non-cyclic strengths and between the material's strength and Young's modulus values (Reference 16), Kairos Power considers that relying on historical data obtained for irradiated and unirradiated medium-grained graphite grades is acceptable to inform on the expected fatigue behavior of ET-10 under irradiation. In other words, graphite grades exhibit similar trends in properties regardless of grain size. This means that a fine grain and a medium grain graphite both exhibit similar changes in fatigue strength under irradiation, although the magnitude of the change may differ. As a result, relying on unirradiated fatigue strength data is conservative compared to the use of irradiated data (Reference 16) up to the point where the irradiated material's cyclic (fatigue) and non-cyclic strengths are no longer greater than the unirradiated material's strength. To Kairos Power's knowledge, no publicly available data at the time of this writing reports fatigue testing results for graphite materials so close to crossover. For example, the observations made for H-451 and PGX do not extend far beyond turnaround. However, fatigue data far beyond turnaround is not needed for KP-X because the qualification envelope discussed in Chapter 4 does not include irradiation conditions that could lead to the case where the irradiated material's strength approaches its non-irradiated counterpart value.

As a result, to demonstrate that ET-10 follows the same trends as H-451 and PGX, Kairos Power will perform low cycle fatigue testing related to thermal transients on unirradiated samples under stress conditions representative of KP-FHR operating conditions. The tests will be designed so as to enable the comparison between ET-10, IG-11 (Reference 17), H-451 and PGX and account for design considerations relevant to the KP-FHR.

In addition, the Division 5 code allowable stress limits are lower than the material's fatigue strength values for a low number of cycles. If so, complying with the 2017 Edition of the Division 5 code remains conservative despite the lack of fatigue specific design criteria. However, if the fatigue test data show that ASME allowable stress limits are higher than the material's fatigue strength, then Kairos Power will adjust allowable stress limits to be conservative. Also, as is discussed further in Chapter 4, irradiation increases the strength of structural graphite, so it is conservative to rely on unirradiated strength data in the estimation of failure probabilities and to derive allowable stress limits.

3.2 PROPERTY VARIATION

Property variation will be evaluated in the license applications for both the non-power and power KP-FHRs using the method described in this section. Graphite has higher property variation than that of metallic materials, even when produced by a well-controlled manufacturing plant and process. The variation of graphite properties mainly comes from the processing method and the ability to implement process control. The objective of this evaluation is (1) to understand the property pattern within the billet; and (2) to establish the baseline for the property consistency throughout years of production. In addition, the lot-to-lot variation data will be used to demonstrate the applicability of the data collected by ORNL, which used ETU-10 in an irradiation campaign, for the qualification of ETU-10 for KP-FHR structural graphite (see Appendix B for a full discussion).

The property variation data discussed in Section 3.2 are provided by Ibiden. The property variation data includes intra billet and inter billet variation based on the billets taken from 3 charges. The analysis of data from Section 3.1 and 3.2 allows a holistic evaluation of ET-10 graphite in terms of its property variation and consistency over the years of production.

Kairos Power will evaluate property variations at two levels, (1) local variation (or billet uniformity) and (2) lot-to-lot variation. Kairos Power will use Ibiden's historical data to evaluate property variation. According to the Division 5 code, HHA-III-5000, *Use of Historical Data*, (Reference 15) if the required test data already exists, new testing is not required. As part of the structural graphite material qualification, Kairos Power will verify that historical data is applicable to the procured structural graphite for a particular license application. Each section of this report that discusses reliance on historical data in the qualification plan discusses how the applicability of the historical data will be verified (See Sections 3.2, Section 4.3, and Section 5.1).

3.2.1 Local Variation

Local variation of ET-10 (billet uniformity or intra billet variation) involves evaluating property gradients introduced by the manufacturing processes. It is a material characteristic rather than quality control issue. Billet uniformity and property pattern of the feedstock graphite billet are used to determine the cutting pattern in production of reflector blocks.

Part of the qualification for structural graphite in a KP-FHR will rely on local variation data from Ibiden. The Ibiden local variation data would be considered historic data that would be evaluated to meet Article HHA-III-5000. Local variation data from Ibiden will be verified against the data collected that is described in Table 6.

Ibiden's local variation data includes 165 specimens, with 55 specimens per slab. This comprehensive dataset (historical data) will be verified by the newly collected data in this qualification program (Section 3.1, Table 6).

Figure 9 shows an example of a billet (ET-10) cutting pattern provided by Ibiden on density and strength variation. The sampling reflects the property gradient in the longitudinal and transverse directions. Figure 10 further illustrates the strength variation within the billet at "upper", "middle" and "lower" positions. The figure shows a typical strength pattern for isostatically molded graphite in which the strength measured from samples at the middle position is lower than the strength measured from samples at the ends. Consistent with industry-wide practice, the property measurements will be conducted at room temperature.

3.2.2 Lot-to-Lot Variation

Lot-to-lot variation involves evaluating property consistency through multiple ET-10 production lots. A "lot" can be made up by multiple graphitization charges depending on manufacturer. From the end-user point of view, lot-to-lot

variation establishes the property baseline and provides indication of any property shifts from the time the material is qualified to the time of purchasing material for a reactor. This evaluation is an extension of the property characterization described in Section 3.1, which is for the [[ ]] sampled from 3 charges. The objective is to monitor the key properties over an extended period of time (e.g., decades). Meaningful lot-to-lot variation has to be obtained from the manufacturer's property database. In fact, the lot-to-lot variation data are obtained by compiling the inspection data of the individual ET-10 billet. For future ET-10 orders, the inspection data can be compared with this lot-to-lot data to see where it is with respect to the property distribution. However, the acceptability of the graphite material is still based on the ET-10 specification determined through the qualification program, discussed further in Section 3.4.

The Ibiden lot-to-lot variation data would be considered historic data that would be evaluated to meet Article HHA-III-5000.The data collected years ago (historical data) can be verified against the data obtained from the recent or current production lot.

Figure 10 is an example dataset provided by Ibiden showing density variation over a 10-year period of ET-10. The properties to be evaluated for lot-to-lot variation are, bulk density, strength, CTE and electrical resistivity. Consistent with industry-wide practice, the property measurements will be conducted at room temperature, except for CTE which is measured at 50-400°C.

The individual property variation over approximately a 10-year span is presented as average value and data distribution within ±1, ±2, ±3 standard deviations of the mean. For example, CTE variation (in WG direction) for the production period from 2009 to 2019 shows the average value of 3.81x10^{-6}/°C based on 553 data points, with standard deviation of 0.214. The majority data are between +/- 1 standard deviation of the average value (e.g., between 3.60 and 4.03), with the minimum value of 3.23, the maximum value of 4.50 for the whole dataset. The data show the practical range of CTE magnitude and its variation for ET-10. Under the qualification plan, Kairos Power would combine this with the data generated in Section 3.1 and modeling results to finalize the CTE specification. This method would be applied for each of the parameters in the MDS in Table 6. See Section 3.4 for further information about how the specification will be defined.

3.3 PURITY

The Division 5 code and ASTM International do not provide a purity requirement for graphite used in a molten salt reactor. ASTM D7219-08 states that high purity nuclear graphite for a gas-cooled reactor should have ash content equal or less than 300 ppm, and an equivalent boron content (EBC) equal to or less than 2 ppm. Kairos Power expects to use [[ ]] ash content and [[ ]] equivalent boron content as a purity requirement for the KP-FHR.

According to Ibiden, the purity of ETU-10 is an ash content ≤5 ppm and ET-10 an ash content ≤ 100 ppm. Based on the full trace element analysis provided by Ibiden, the calculated EBC is 0.22 ppm for ETU-10. Kairos Power confirmed ET-10 purity for recently purchased material. The results show that the average ash content is 77 ppm (Ibiden's inspection results) and average EBC of 0.77 ppm (Kairos Power's test results). The results indicate that both ETU-10 and ET-10 satisfy the purity requirement as specified in the ASTM D7219-08. Kairos Power will finalize the ET-10 purity specification using the ASTM D7219-08.

Table 8 shows an example of the full element analysis of ET-10 by Glow Discharge Mass Spectrometry (GDMS). The results indicate that the purity of ET-10 is high and most elements are below the detection limit. Kairos Power will determine the upper limit of elements that could affect the ability of the graphite reflector to perform its safety function in the qualification program as follows:

- The neutron absorbing elements will be limited by ensuring that the calculated EBC is not greater than 2 ppm.
- The upper limit of elements that could potentially accelerate oxidation of graphite will be finalized based on the oxidation test results. See Section 5.3 for more information about the oxidation tests.

Other impurity categories related to activation, metallic corrosion and fissile or fissionable elements do not affect the ability of the reflector to perform its safety function. Further, the effect of impurities on post-operation considerations is not related to the structural graphite material qualification, or the material's safety function.

3.4 DEFINING A STRUCTURAL GRAPHITE SPECIFICATION

One of objectives in this qualification program is to determine the as-manufactured graphite ET-10 specification, which will be used as accept/reject criteria for the future ET-10 graphite ordering for material to be used in a KP-FHR. The specification includes the mechanical and thermal properties, as well as purity.

The process to determine the specification of mechanical and thermal properties is recapped below.

- The intra-billet and inter-billet properties and their variations collected in Section 3.1 provide the range of each property of ET-10 graphite. The property values will be used as input for the analysis described below.
- The strength data collected in Section 3.1 will be used for deriving allowable stress limits and estimating failure probabilities that are consistent with Article HHA-3000 of the Division 5 code. Variations observed for the material properties listed in Section 3.1 will inform sensitivity analyses aimed at assessing the influence of such variations on predicted stress levels and failure probabilities.
- The acceptance criteria for the properties will be chosen to meet the allowable stress limits and probabilities of failure. The acceptance criteria will be used for decisions about acceptance or rejection of material to be used in a KP-FHR.

The purity specification of ET-10 will be determined based on the purify requirement specified in the ASTM D7219-08. Kairos Power will finalize the ash content and EBC as well as upper limit of individual elements impacting safety function of structural graphite through the qualification program.

4 QUALIFICATION OF GRAPHITE UNDER IRRADIATION

4.1 IRRADIATION ENVIRONMENT

The power reactor graphite reflector will operate normally at temperatures between approximately 550°C at the bottom and 700°C or less at the top – a representative temperature distribution is shown in Figure 12. The design limit temperature is 816°C for a short duration during postulated events. The fast neutron flux reaching the side reflector's exposed surface is rapidly thermalized within the reflector, thereby decreasing by about one order of magnitude every [[ ]], as shown in the representative map of Figure 12. Only the first [[ ]] of the graphite reflector will receive significant fluence leading to appreciable property and dimensional changes. The maximum fast flux within the side reflector will occur at mid-height at the reflector surface and will be approximately [[ ]] , equivalent to [[ ]]. The non-power reactor (5-year component life) is expected to see smaller fluence levels than the power reactor ([[ ]] component life) and the irradiation temperature range for the non-power reactor will be bounded by the temperature range of the power reactor.

4.2 ASME IRRADIATION QUALIFICATION REQUIREMENTS FOR STRUCTURAL GRAPHITE

The Division 5 code, Article HHA-3142.1, considers any graphite exposed to fluences greater than 0.25 dpa to be "irradiated graphite." The following properties, separated into basic properties and irradiation creep properties, should be measured on the selected graphite grade (per HHA-2200, *Material Properties for Design* and *HA-III-3000 Properties to be Determined*).

4.2.1 Basic Properties

- Irradiation-induced dimensional change: This is the change in length, normalized to the initial length expressed as a percentage.
- Irradiation-induced change in coefficient of thermal expansion: This is expressed as a value normalized to the as-manufactured value. The temperature dependence of this property shall be determined.
- Irradiation-induced change in strength: This is expressed as a value normalized to the as-manufactured value and shall be based on a strength parameter selected by the Designer. Note that irradiation-induced change in strength need only be measured should the Designer desire to account for the strength increase at low or intermediate damage doses.
- Irradiation-induced change in elastic modulus: This is expressed as a value normalized to the as-manufactured value.
- Irradiation-induced change in thermal conductivity: This is expressed as a value normalized to the as-manufactured value. The temperature dependence of this property shall be determined.

4.2.2 Irradiation Creep Properties

- Irradiation-induced creep coefficient: The creep coefficient to be used is to be the coefficient (or set of coefficients) required for the irradiation creep model proposed for use by the designer.
- The effect of creep strain on coefficient of thermal expansion and elastic modulus shall be determined.

For irradiated graphite, a viscoelastic analysis shall be used to calculate irradiation-induced internal stresses. The Division 5 code does not specify the analysis method, model, or framework to be used for this analysis.

The Division 5 code (HHA-III-3000, *Irradiated Graphite*, and HHA-II-4000, *Detailed Requirements for Derivation of the Material Data Sheet — Irradiated Material Properties*) also specifies the following additional requirements for irradiation qualification of the structural graphite:

- The temperature range of material in operation in the reactor for all service levels shall be enveloped by the temperature range of the data
- Maximum temperature increments of 200°C shall be used
- In near-isotropic graphite grades such as ETU-10 (CTE isotropy ratio comprised between 1.1 and 1.15 per ASTM D7219), the irradiation-induced changes in properties such as strength, thermal conductivity, linear coefficient of thermal expansion, and elastic modulus need not be measured for both grain orientations
- For irradiation-induced linear dimensional changes, both grain orientations shall be characterized for near-isotropic graphite materials such as ETU-10

4.3 IRRADIATION QUALIFICATION PROGRAMS

The irradiation qualification programs for both reactors are described below. Both programs rely on three types of data:

- Historical data: ASME-required basic properties data for ETU-10 for a range of irradiation temperatures and fluences have been collected by ORNL (Reference 9) – they are summarized in Table 9 and depicted in Figure 13. Appendix B provides information about the applicability of the ORNL dataset (Reference 9) to the ET-10 structural graphite that will be used in the non-power and power reactors.
- Existing/literature data: literature data on irradiation creep in graphite will be used for graphite qualification for the non-power reactor
- Additional data: new irradiation creep data on ET-10 will be generated for graphite qualification for the power reactor

The methods to calculate the corresponding qualification envelopes based on these different sets of data are described. The calculated qualification envelopes will be described and shown to envelope the reactors' operating conditions at the time of the license application. Transient conditions would not need to be bounded by the irradiation qualification envelopes as no significant fluence will be accumulated during transient events. Kairos Power seeks approval for the methods to define qualification envelopes for irradiation effects on structural graphite material properties, as part of the qualification plan. The existing ORNL dataset contains dimensional change measurements, which will be used to estimate the turnaround fluence with confidence intervals. Schematics of envelopes and how they relate to expected ranges of operating conditions and to the historical ORNL data are given for illustration only in Figure 14.

4.3.1 Irradiation Qualification Envelope and Program for a Power KP-FHR

4.3.1.1 Basic properties

The irradiation qualification program for the power reactor conforms to the Division 5 code for data requirements on basic properties. ASME-required basic properties data for ETU-10 at several irradiation temperatures and fluences have been collected by ORNL (Reference 9). The ORNL data is plotted as a point cloud in Figure 13. Each point represents the fluence/temperature pair reported by ORNL for which basic properties were measured. Appendix B provides information about the applicability of the historical ORNL dataset (Reference 9) to the ET-10 structural graphite that will be used in the non-power and power FHR.

The ORNL data was generated using ASTM standards for all the measurements. In particular, all the standards required by ASTM C781 were used, as detailed in ORNL/TM-2014/86 (Reference 19) except in two cases: for

measurement of modulus of elasticity, where a more general standard for ceramic is cited (although the method is similar); and for strength where the size constraint for irradiation specimens required the use of equibiaxial testing, for which the relevant ASTM C1499 was used. In addition, while ASTM C625 on the standard practice for reporting irradiation results on graphite is not cited in the ORNL reports, it only recommends that certain information is included in reports. Four reports and one detailed Excel spreadsheet have been issued by ORNL on the irradiation campaign for ETU-10, with great details on all the information categories mentioned in ASTM C625.

Graphite strength was only measured in one direction (WG) by ORNL. This is consistent with the Division 5 Code, Article HHA-II-4000, which states that changes in properties like strength are to be reported in the form of the relative change from the value before irradiation and as a function of the fluence over the relevant operating temperature range. The article also states that distinction with respect to the preferred grain orientation is not required when reporting fractional change of certain properties, including strength, for near-isotropic graphite grades. To account for strength anisotropy in models, Kairos Power will rely on the fact that the response of strength to irradiation is analogous to Young modulus's modulus response (Reference 20). The analogous behavior was shown for IG-110 to fluences post-turnaround and pre-crossover (Reference 21). ETU-10's irradiated Young modulus' data is available and the ratio of with-grain to against-grain will be used to estimate the irradiated strength in the against-grain direction from the measured with-grain direction.

The qualification envelope for basic irradiation properties will be based on the ORNL irradiation data. An envelope will be defined for each of the five measured properties. The method to calculate each envelope will be as follows:

- Define the convex hull envelope for the ORNL data (i.e., the smallest convex set that contains the data). The convex envelope for dimensional change is shown in Figure 15.
- Fit a regression model of the property as a function of both fluence and temperature. The model will be a closed form function (e.g., a polynomial), and the number of parameters selected to avoid overfitting. Statistical methods will be used to explore the uncertainty in the model parameters (bootstrapping and Bayesian methods) that account for uncertainties in each fluence, temperature, and measurement (see Appendix C).
- Show that the uncertainty of the fit (e.g., 95% confidence interval), accounting for uncertainties in fit parameters, within the convex hull is below an acceptable value and that 'cliff-edge' effect (i.e., sudden change of behavior) are not expected within the hull.

4.3.1.2 Irradiation creep properties

The irradiation qualification program for the power reactor will measure irradiation creep properties for ET-10. The objective of the irradiation creep test will be to calibrate an ET-10 irradiation creep model. The irradiation creep testing will have the following features:

- <u>Test material</u>: ET-10 in the WG orientation. The justification to measure in only one direction is as follows: The influence of direction (AG, WG) on irradiation creep in graphite is well known and captured by the inverse dependence of the steady-state creep coefficient on Young's modulus (Reference 24). As such, the creep coefficient measured in the WG direction can be used to estimate the creep coefficient in the AG direction. If an isotropic creep model were to be used, using the steady-state creep coefficient measured in the WG orientation (higher Young's modulus hence lower creep coefficient) would be conservative for stress analysis as a smaller creep coefficient entails less stress relaxation.
- <u>Irradiation capsule design</u>:
  - Stressed and un-stressed specimens will be irradiated at the same time and in temperature and flux conditions as similar as practical.

    - Stressed specimens will be loaded by application of a dead weight, a bellow apparatus, or using restrained shrinkage.

- <u>Irradiation temperatures</u>:
    - Two target test temperatures at 500°C and 700°C will be selected to bound operating conditions with the maximum 200°C allowed by ASME.
    - The desired test irradiation temperatures will be achieved by careful design of gas gaps within capsules.

- <u>Irradiation fluences</u>: The target fluence ranges will be 10-15 x 10^{21} n/cm^2 (E>0.1 MeV) and 20-30 x 1021 n/cm2 (E>0.1 MeV), corresponding to about 7-10 years (pre-turnaround) and 13-20 (post-turnaround) full power years, respectively. The ranges occur because the samples are arranged axially in the material test reactor core. For example, HFIR has a 20" active core length, with the top and bottom of that length reaching ~70% of the peak neutron flux. As such, if specimens reach 10 dpa in the center of the core, the specimens at the extremities would reach 7 dpa.

- <u>Applied stress</u>: For the stressed specimens, a compressive stress of [[ ]] will be used.

- <u>Test matrix</u>: [[ ]] specimens per condition (fluence, temperature, stress/no stress) will be tested. See Table 10. This number of specimens is consistent with best practices:

    - the AGC campaign (Reference 30) used 10 and 4 specimens for IG-110 per fluence level, load, and temperature, in the WG and AG directions, respectively. Only one temperature was tested, while Kairos Power will test two temperatures.

    - Oku's work (Reference 26) on IG-110 used 7 specimens per fluence (range), temperature, and load (although 21 specimens were used for the unloaded condition). Only one temperature was tested, while Kairos Power will test two temperatures.

    - ORNL's work on IG-110 (Reference 69) used 5 specimens per fluence level, load, and temperature.

    - NRG at the Petten test reactor typically uses 12 specimens for one temperature or 6 specimens for two temperatures, per fluence and load (Reference 70).

- <u>Post-irradiation examination</u>:
    - Creep strain will be measured by measuring dimensional changes in stressed and un-stressed specimens (see Section 4.3.2).
    - The irradiation creep testing will be able to detect if tertiary creep occurs through a substantial increase in creep rate. If tertiary creep is expected to happen in the power reactor lifetime (which will be bounded by irradiation creep testing conditions), it will be accounted for in an irradiation creep model.
    - The effect of creep strain on CTE and Young's modulus will also be measured, as required by Division 5.

The qualification envelope for irradiation creep properties in the irradiation temperature/fluence space will be defined by the measured irradiation temperature and fluence. Assuming the target temperature and fluence from Table 10 are reached, the irradiation creep envelope will be 500°C to 700°C irradiation temperature and 0 to 20-30 x 10^{21} n/cm^2 (E>0.1 MeV) fluence.

4.3.2 Irradiation Qualification Envelope and Program for a Non-Power KP-FHR

4.3.2.1 Basic properties

The irradiation qualification program for the non-power reactor conforms to the Division 5 code for data requirements on basic properties. The qualification data for basic properties will be the same as for the power reactor and the method to define the qualification envelope will also be the same. Appendix B provides information about the applicability of the historical ORNL dataset (Reference 9) to the ET-10 structural graphite that will be used in the non-power and power FHR.

4.3.2.2 Irradiation creep properties

The qualification plan for irradiation creep for the non-power reactor will use existing data to define creep coefficients. This is justified because the end-of-life fluence for the side reflector falls before the turnaround fluence, which has two implications. First, graphite component end-of-life is generally considered to lie between turnaround and crossover (Reference 22). Therefore, an irradiation-induced stress-driven failure of the graphite would not be expected to happen within a pre-turnaround component life. Stress and failure analysis of the graphite blocks will be conducted to confirm this conclusion. Second, for pre-turnaround fluence and at temperatures below 700°C, irradiation creep behavior among all graphite grades can be captured by a simple creep model (References 23, 24, and 25). This can be demonstrated by compiling a large set of existing irradiation creep data from the literature and fitting the simple model to the data. The simple model is defined as:

$$\varepsilon_T = \varepsilon_P + \varepsilon_S$$

$$\varepsilon_p = \frac{\sigma}{E_0}$$

$$\varepsilon_s = K\sigma E_0$$

Where: ε is the creep strain for total, T, primary, P, and secondary, S, in %. σ is the applied stress, in MPa. γ is the fluence. K is the secondary creep coefficient. The primary creep coefficient is also called the ratio of the maximum transient creep strain to the initial elastic strain and has been measured as close to 1. (Reference 24).
The primary creep coefficient can be estimated from the intercept of the creep strain curve when plotted against fluence (Reference 26).

The compilation of data is extracted from experiments with direct loading and out of core measurements (no restrained shrinkage). Creep data is only considered in the orientation parallel to the applied load and no lateral creep data has been analyzed. Due to the multiple different origins and long periods of time between the irradiation creep experiments, several assumptions have to be made in order to compare the data on a like-for-like basis. Experiments have been chosen where the data is readily available in open literature and are as follows:

- H-327 and H-451 graphite grades irradiated at Oak Ridge National Laboratory (ORNL) at 600 and 900°C. Also referred to as the "OC" series (Reference 26).
- ATR-2E graphite grade irradiated at the High Flux Reactor (HFR) at Petten, Netherlands, at 300, 500 and 550°C. Referred to in this report as "Haag" (Reference 28).
- IG-110 graphite grade irradiated at the Japan Material Testing Reactor (JMTR) at ~750 to 1000°C. Referred to in this report as "Oku" (Reference **Error! Reference source not found.**).
- Molded grades (IM1-24, VNMC and SM2-24) irradiated in the PLUTO reactor at 850 and 1050°C. Referred to in this report as "PLUTO" (Reference 29).

- Various grades (NBG-17, NBG-18, PCEA, IG-110, 2114, H-451 and IG-430) in the Advanced Graphite Creep (AGC) experiment irradiated in the Idaho National Laboratory Advanced Test Reactor at ~600 and ~800°C. Referred to in this report as "AGC" (Reference 30).
- AGOT, H-337 and AXF-8QBGI graphite grades irradiated in the Idaho Engineering Test Reactor (ETR) at 550 and 800°C. Referred to in this report as "Gray" (Reference 31).
- H-451 graphite grade irradiated in the Oak Ridge Research Reactor (ORR) at 900°C. Referred to in this report as "Burchell" (Reference 32).
- Isotropic extruded grades irradiated in the BR2 test reactor at 300 to 600°C. Referred to in this report as "BR2" (Reference 33).

A summary of the experimental conditions is provided in Table 10. Additionally, a list of the nuclear graphite grades and a brief description of their type and manufacturer process is provided in Table 12 where the information is available in open literature.

Figure 16 shows the extracted secondary creep coefficient K from these datasets as a function of irradiation temperature. It also shows the UKAEA irradiation creep model (Reference 34) which considers a constant K up to 700°C and a temperature dependence for K above ~700°C. This compilation of data will be further analyzed to quantify a best estimate and confidence intervals for the creep coefficient in pre-turnaround conditions, which will be used for ET-10.

The qualification envelope for irradiation creep for the non-power reactor will be defined by the temperature-dependent estimate of the turnaround fluence. The existing ORNL dataset contains dimensional change measurements for ETU-10 in the WG and AG grain directions and volume change, which will be used to estimate turnaround fluences. As detailed in Appendix C, the turnaround fluence will be estimated by fitting a two-dimensional (surface) model of the dimensional change as a function of the irradiation temperature and fluence. A polynomial functional form will be used, with the number of parameters minimized to prevent overfitting. On the fitted model, the temperature-dependent turnaround fluences are defined as the valley of minimum dimensional change, which can be estimated analytically from model parameters. The uncertainty in the turnaround fluences will be estimated from uncertainties in the model parameters calculated using the two statistical methods described in Appendix C and a confidence interval will be proposed. The smallest turnaround fluence for volume change of the two methods will be used to define the envelope. Additional variabilities in turnaround fluence caused by unirradiated graphite within-billet and between billets will be considered (See Appendix C). This will be compared to the maximum fluence at any location for the KP-FHR non-power reactor to verify that no portion of the graphite reflector will exceed this conservative turn-around fluence limit.

5 DEMONSTRATION OF ENVIRONMENTAL COMPATIBILITY

5.1 INTERACTION OF GRAPHITE AND FLIBE

The Flibe-graphite interaction evaluation described in the Division 5 Code, Article HHA-B, "Environmental Effects" is non-mandatory. However, the graphite reflector is a safety-related component in the reactor and the Flibe coolant is a unique material.

Kairos Power conducted a literature review of the information available about interactions between Flibe and graphite. This section discusses the potential phenomena that could potentially affect the properties of structural graphite due to its interaction with a molten salt. These phenomena, listed below, were identified through the phenomena identification studies discussed in Section 2.3, and additional literature review conducted by Kairos Power staff. There are no other known degradation mechanisms for structural graphite in a molten salt environment.

- Chemical Factors
  - Fluorination/Intercalation (See Section 5.1.3)
  - Chromium carbide formation (See Section 5.1.3.1)
  - Oxidation (See Section 5.3)
- Physical Factors
  - Infiltration (See Section 5.1.1)
  - Stress (See Section 5.1.2)
  - Erosion and Abrasion (See Section 5.2)

Because graphite is buoyant in Flibe and because Flibe remains liquid in the design basis (normal operation and postulated events), the molten salt does not impart stress on the structural graphite. Stress would be necessary to affect the mechanical performance of the graphite reflector structure. Therefore, stress imparted on the structural graphite from infiltrated or surrounding Flibe is not considered a credible degradation phenomenon for a KP-FHR and is out of scope for this qualification plan.

In most cases, literature data exist to demonstrate the compatibility of structural graphite with Flibe for most environmental compatibility phenomena. This section also describes a few limited phenomena for which Kairos Power proposes to conduct additional testing to demonstrate compatibility of structural graphite in a Flibe environment.

This section discusses the interaction of Flibe and structural graphite in the reflector. For more information regarding interaction between Flibe and graphite for the fuel pebbles, see the Kairos Power topical report titled *KP-FHR Fuel Performance Methodology* (KP-TR-010, Reference 35). Qualification of the graphite used in fuel pebbles is not in the scope of this report.

5.1.1 Molten Salt Infiltration in Graphite

Flibe molten salt does not wet graphite (Reference 36) under the operating conditions in a KP-FHR and, therefore, Flibe is not expected to infiltrate into graphite without the presence of sufficient differential pressure between the Flibe and the pore pressure. In Washburn's model, infiltration occurs when the pressure difference is greater than a threshold pressure given by (Reference 37):

$$p = -4\gamma\cos\theta/d \qquad \text{(Equation 5.1)}$$

In the equation p is the threshold pressure, γ is the Flibe surface tension, d is the entrance pore diameter, and θ is the contact angle for Flibe on graphite.

The equation can be used to estimate the threshold pressure for Flibe infiltration into graphite. As discussed in Section 3, ET-10 and ETU-10 have the same physical properties, and the infiltration data and pore structure data measured based on ETU-10 apply to ET-10, and vice versa. Literature data provides a Flibe surface tension of [[ ]] at 650°C (Reference 38) and a contact angle, [[ ]] at 500-800°C (Reference 39). Based on that literature data, the relation of the threshold infiltration pressure to the entrance pore size is established per Equation 5.1, as shown in Figure 17. Using the entrance pore diameter of ETU-10 grade graphite measured by ORNL, [[ ]] (Reference 40), the threshold pressure for ETU-10, as well as ET-10, is [[ ]], see Figure 17. In a KP-FHR, the Flibe hydrostatic pressure is highest at the bottom of the vessel. This is the pressure that may cause Flibe infiltration, i.e., infiltration pressure.

In a KP-FHR non-power reactor, with a fluid height around 4 m, the corresponding infiltration pressure will remain below the threshold infiltration pressure, [[ ]]. According to the estimation from Figure 17, the infiltration is not expected if the infiltration pressure is below the threshold value [[ ]]. Moreover, the KP-FHR non-power reactor is planned to operate before reaching turnaround. Before turnaround, the graphite volume shrinks with fluence, which is accompanied by a decrease of porosity. Therefore, Flibe infiltration, if it occurs, will not increase during the planned duration of the non-power reactor operations.

In a KP-FHR power reactor, assuming a fluid height of up to 6 m , the infiltration pressure is estimated to be [[ ]] which will be greater than the threshold value, [[ ]]. Therefore, Flibe infiltration is possible. Additionally, the KP-FHR power reactor is planned to operate beyond turnaround. Before turnaround graphite porosity and pore volume would decrease with fluence. At turnaround, the effect would begin to reverse. Beyond turnaround, the graphite porosity and pore volume would then increase, with the associated increase in Flibe infiltration. However, even if Flibe infiltrates into graphite, molten Flibe will not affect graphite's integrity under KP-FHR operating conditions or postulated events. See Section 5.1.2 for a discussion of that conclusion.

There are no known mechanisms for molten salt that has infiltrated into graphite to affect graphite mechanical integrity in a KP-FHR. However, Kairos Power will conduct tests of molten Flibe infiltration into ET-10 graphite to confirm that Flibe infiltration does not affect the mechanical properties of ET-10. The Flibe infiltration test plan is discussed in Section 5.1.1.1.

5.1.1.1 Flibe Infiltration Test Plan

The molten salt infiltration test will follow the guidance provided in ASTM D8091-16. Kairos Power will fabricate the infiltration test unit to fulfill the requirements to perform Flibe infiltration and to quantify the amount of Flibe infiltrated into ET-10. The infiltration test unit will be designed based on Kairos Power's experience handling molten Flibe. The key components of the infiltration test unit include:

1. An autoclave, allowed to be operated at pressure up to 1000 kPa, temperature up to 900°C
2. A heating system with temperature control to match the requirement for the autoclave
3. A sample holder and a crucible made of graphite, to avoid potential contamination from stainless steel autoclave in the Flibe environment
4. A sample lifting device, which allows the sample holder to be moved in and out of molten salt under the pressure
5. An Ar pressure tank to provide pressure needed for experiments
6. A glovebox able to handle Flibe infiltrated samples

The thermal gradient and the pressure gradient in the reactor are roughly in opposite directions, see Figure 18 for an illustration of the gradient directions. The hydrostatic pressure in the vessel means that the pressure is higher at the bottom of the reactor than at the top. As discussed in Section 5.1.1, for Hermes, the pressure at the bottom of the reactor remains below the threshold infiltration pressure. Therefore, no Flibe infiltration is expected in a KP-FHR non-power reactor. For the power reactor, infiltration could occur in approximately the bottom third of the reactor, but not at the top of the reactor where the highest temperatures are seen. Although pressure is the main driver to cause Flibe infiltration, higher temperatures also promote infiltration due to the reduced surface tension of molten salt. The highest temperature of the power reactor is 700°C at the top of reactor. To be conservative, Kairos Power will conduct the Flibe infiltration testing at 750°C. The infiltration pressure will vary from 100 to 500 kPa. 500 kPa is roughly 2.5 times greater than the pressure at the bottom of the power reactor, so the pressure range is conservative.

Based on the above discussion, the test matrix for infiltration is developed to include pressure, temperature, and infiltration duration for each test run as listed in Table 14. The pressure step is selected: (1) to bound the KP-HFR designed operation pressure with margin; (2) to obtain the threshold pressure for Flibe infiltration to ET-10 and (3) to determine the pressure causing full infiltration, i.e., the amount of Flibe infiltration corresponding to the maximum infiltration. Infiltration durations of [[ ]] will allow the system to reach equilibrium (Reference 37).

The amount of Flibe infiltration will be calculated using the formula below.

$$wt\%\ Flibe\ infiltration = \frac{sample\ weight\ after\ infiltration - sample\ weight\ before\ infiltration}{sample\ weight\ before\ infiltration} \times 100$$

Regarding the graphite test sample preparation and selection, the following points are considered:

- The sample dimensions will allow for use in both infiltration tests and strength tests after the infiltration.
- Any synthetic grade graphite including ET-10 has property variation within the same billet. To obtain more conservative results, the sample with lower density will be used. Because the lower density portion has higher porosity and may have larger pore size, it will have a lower threshold infiltration pressure, i.e., more Flibe infiltration.

Molten salt infiltration behavior, e.g., threshold pressure, amount of infiltration, is a reflection of a graphite's pore structure (pore size and its distribution). Pore size and distribution are not used as parameters in the design of the graphite reflector structure, therefore pore size and distribution will not be parameters characterized in the material qualification program for ET-10.

5.1.2 Effect of Molten Salt Infiltration on Graphite Mechanical and Thermal Properties

The effect of molten salt infiltration on the graphite mechanical properties was investigated by Zhang et. al, in a project to develop a similar molten salt reactor to KP-FHR but using different type of solid fuel (References 41 and 42). FLiNaK was used as the molten salt. Two superfine grain graphite grades, one of which was IG-110, were used as test samples. See Appendix D for an evaluation of IG-110's applicability to the qualification of ET-10.

The authors first infiltrated the graphite with molten FLiNaK at different infiltration pressures and obtained a series of samples with different amounts of salt infiltrated. Then, the authors conducted strength tests at room temperature and at 700°C on the infiltrated samples. The results observed at room temperature and at elevated temperature show different trends (References 41 and 42). At room temperature, the strength of the infiltrated graphite showed a 30-40% increase. This was attributed to the composite effect, that is the solid salt acted as reinforcement. However, the strength measurements subsequently taken at 700°C were found to be reduced by 10-20%. As shown in Figure 19, the strength decreases as the amount of salt infiltrated increases. The difference is

that the sample measured at elevated temperature (at 700°C) went through a freeze-thaw cycle; the sample was cooled from infiltration temperature to room temperature, then reheat to 700°C. The mechanism causing the strength reduction is discussed below.

In addition to the strength, the effect of FLiNaK infiltration on the thermal expansion was also investigated (References 43). The results explain the mechanism of strength reduction observed previously. Figure 20 shows the thermal expansion of six graphite samples with FLiNaK infiltration amounts ranging from 7.2% to 17.1%. The infiltrated samples all show a higher rate of thermal expansion (CTE) than that of virgin samples when measured between room temperature and ~450°C (FLiNaK m.p. ~450°C), and the rate is then back down to the same rate as virgin sample from 450°C to 700°C. However, the thermal strain (dL/L_0 %) of salt-infiltrated graphite remains higher than that of the corresponding virgin graphite sample. The results indicate that the deformation as a result of salt infiltration is irreversible. The irreversible deformation is an indication of the internal structure damage, which could account for the reduction in strength. The effect is more significant for the samples with greater amount of salt infiltration for all the fine grain graphite grades. The authors concluded that the deformation is caused by CTE mismatch between salt and graphite (about 10x) (References 43 and 44). In the same papers (References 43 and 44), the CTE of graphite was observed to be unaffected when salt is in liquid state. The results of this study indicate that a freeze-thaw cycle can affect the measured strength of infiltrated graphite.

As discussed in 5.1.1, molten salt infiltration behavior is determined by the pore structure of graphite, e.g., entrance pore diameter and pore volume. IG-110 and ET-10 have similar pore structure (see Appendix D), therefore, it is reasonable to use the results from IG-110 to predict ET-10 behavior for these effects. In terms of the salt (Flibe vs FLiNaK), the mechanism of transferring the stress from solid salt to graphite due to the CTE mismatch is the same. So, the results in the studies mentioned above using FLiNaK is applicable to the Flibe-graphite system.

In summary, it is expected that salt infiltration can damage the graphite structure and reduce its strength only if a freeze-thaw cycle occurs. Since KP-FHR is not expected to experience a freeze-thaw cycle during postulated events or normal operation, no reduction of graphite strength is expected even if some salt infiltrates into graphite. No change in CTE of graphite was observed if salt is in liquid state. There are no other known mechanisms for physical degradation related to salt infiltration. Nevertheless, testing outlined in section 5.1.2.1 will provide confirmation of that salt infiltration alone does not degrade the mechanical strength of graphite.

5.1.2.1 Validation test of the effect of Flibe infiltration on graphite mechanical property

To further confirm the analysis conducted in 5.1.2, Kairos Power will conduct validation tests on the effect of Flibe infiltration on graphite mechanical properties. The test will take a different approach than what is mentioned in the literature, which convoluted by the effect of infiltration with the effect of phase change for the Flibe. The tests conducted to support the qualification plan in this report will remove salt after infiltration, then measure the strength of graphite only, instead of graphite-salt composite. Thereby, any change in graphite properties due to the molten salt infiltration can be identified. ORNL is developing the test method using FLiNaK molten salt. Kairos Power will apply the same method to a Flibe molten salt graphite system.

The test plan is similar to Flibe molten salt infiltration test discussed in section 5.1.1.1, but only for preparation of a sample to test strength. For the purpose of investigating the effect Flibe infiltration has on the strength of graphite, a conservatively high infiltration pressure will be used, e.g., [[ ]] . After infiltration, the infiltrated salt will be removed by reducing cover gas pressure when the sample is lifted out of molten salt. The residual Flibe trapped in the graphite pore structure will be washed away with dilute HF solution followed by washing with deionized water and drying. The weight change of sample, to initial weight, after Flibe being removed will be used to confirm the completeness of salt removal.

The test matrix is listed in Table 15. The Flibe infiltration conditions are so selected that the amount of Flibe infiltrated can be obtained from the infiltration test (in Section 5.1.1.1) conducted under the same conditions. The compressive strength tests of two groups of samples, pristine and infiltrated, will be conducted. The comparison of strength of ET-10 before and after Flibe infiltration will determine if Flibe infiltration affects graphite strength and the magnitude of that effect.

5.1.3 Chemical Compatibility of Fluoride Molten Salt with Graphite

During the MRSE program in the 50-60s, the chemical compatibility between the graphite and fluoride salt was investigated and found that they were compatible (Reference 45). Flibe molten salt with UF_4 was used, and CGB grade graphite was selected in the MRSE program due to its resistance to molten salt infiltration. The most convincing results so far is from the examination of the decommissioned MRSE reactor after 3 years of operation, which showed no obvious erosion signs and the original machining marks on graphite parts were still clearly visible (Reference 46). The results indicated that no chemical degradation of the graphite occurred. Chemically, the compatibility of CGB grade graphite would be the same as that of ET-10, as discussed further in Section 5.1.3.2.

More recently, two studies reported that graphite fluorination in fluoride salt may occur (References 47 and 48). To confirm whether or not the recent reported results apply to KP-FHR case, an in-depth analysis of the literature results was conducted, and results are highlighted below.

Yang, et al., and Wu, et al., (References 47 and 48) reported the fluorination on graphite when it contacts fluoride molten salts (Flibe or FLiNaK) based on the surface analysis results, mainly from X-Ray Photoelectron Spectroscopy (XPS) and X-Ray Absorption Near Edge Structure (XANES) spectroscopy analysis. The fluorination they observed can be categorized as three possible mechanisms: (1) fluorination through hydrocarbon structure and oxygen functional groups, (2) fluorination on defects in graphite, and (3) intercalation. The potential impact to the graphite structure by the fluorination was summarized in Table 16.

It is well known that hydrocarbon structure and oxygen functional groups are not thermally stable during high temperature processing in graphite fabrication (Reference 49), and that they do not exist at a significant level in bulk synthetic graphite. Fluorination on defects at graphite edge planes was observed at a trace level by X-Ray Photoelectron Spectroscopy (Reference 48). Based on these literature references, no significant bulk effect is credible for the first and second mechanisms listed in the previous paragraph for the structural graphite in a KP-FHR.

Graphite intercalation is the only fluorination mechanism that could lead to structural damage in a KP-FHR through an exfoliation mechanism. Results from Wu et. al (Reference 48) indicate the possibility of fluorine intercalation, but the signal strength was too weak to be confirmed. A more reliable result for the absence of intercalation comes from Bernardet, et al. (Reference 50). Bernardet, et al., maximized the salt/graphite reaction surface by grinding graphite to a powder before impregnating it with a Li, Na, Zr-based fluoride molten salt at 500°C for 60 hours. The results showed that the *c* lattice parameter increased from 6.758 to 6.771 Å after treatment. The increase is not large enough to confirm the formation of fluorine intercalated compound. A typical reported value of graphite interlayer spacing for stage-1 fluorine-intercalated compound is 9.38-9.44 Å and for stage-2 is 12.7Å (Reference 51), which is clearly well above any difference observed from these previous experiments attempting to measure intercalation. He, et. al, investigated the chemical compatibility between FLiNaK and six of graphite grades ranging from superfine grain to medium grain, including IG-110 (Reference 52). The X-Ray Diffraction results demonstrated no formation of graphite intercalation compound even with 17% FLiNaK infiltrated. The MRSE program also studied intercalation of fluorides with graphite and found no indications of intercalation with, or other damaging effects on, the graphite

(Reference 53). In conclusion, graphite intercalation not a concern for the KP-FHR, and no further testing is proposed as part of this program.

In summary, graphite fluorination was observed in fluoride salt, but no fluorine intercalation was observed. Intercalation is the only type of fluorination of concern for degradation since it can cause exfoliation. Some inconsequential amount of fluorination may occur on the defects of graphite edge planes. If any occurs, Flibe-induced graphite fluorination is not expected to impact graphite structural integrity. In addition, Kairos Power will characterize the graphite surface in contact with Flibe molten salt to confirm that no significant degradation occurs related to chemical compatibility with Flibe.

5.1.3.1 Chromium Carbides

Chromium carbides can form on graphite surfaces as a dense film in fluoride molten salt. Literature results found that the carbide formation element, e.g., Cr, does not penetrate into graphite pore structures (Reference 54). Based on the results from the same literature, Kairos Power estimates that roughly 3.5µm of ET-10 graphite is consumed to form a 10 µm chromium carbide (Cr_7C_3) film on an ET-10 graphite surface. The consumption of graphite is a trace amount compared to the mass of the overall graphite reflector. Based on the literature results, the chromium carbide formation is on the graphite surface and the amount of graphite consumption is negligible compared to the thickness of the reflector structure. Therefore, potential chromium carbide formation on the graphite surface will not affect graphite structural integrity. Note that the potential impact of carbide formation on stainless steel material qualification is out of scope for this topical report.

5.1.3.2 Chemical similarities between ETU-10, IG-110, and CGB Grades of Graphite

The chemical reaction between Flibe molten salt and graphite, if any, is mainly determined by the graphite's crystalline structure rather its physical properties, bulk structure, or trace impurities. CGB, IG-110 and ET-10 are all synthetic graphite grades that use coke and pitch as raw materials and a final graphitization process. In the graphite industry, they are treated as the same class of material in terms of their crystalline structure. With respect to the chemical behavior of these graphite grades, the reaction sites in the internal structure are at the edge plane, which is essentially the same structure for each grade. Therefore, CGB, IG-110 and ET-10 grades of graphite would behave similarly with respect to chemical behavior and reactions with Flibe molten salt. Therefore, the information from the studies listed in Section 5.1.3 which contain test data for IG-110 and CGB can reasonably be applied to the understanding of chemical compatibility of ET-10 with Flibe.

5.1.4 Effect of Infiltration on Neutronics

Kairos Power considered the potential for infiltrated Flibe to exit the reflector during a postulated event, resulting in a rapid insertion of reactivity into the core. This scenario is considered not credible for the KP-FHR. Graphite infiltration can be influenced by changes in pressure and wetting angle of Flibe on graphite. The change in either parameter would need to be rapid (on the order of seconds) to insert reactivity fast enough to represent a safety-significant transient.

Under the postulated event conditions for the technology (no vessel ruptures), [[

]]. Therefore, the effect of pressure change in postulated events is negligible and does not represent a source of reactivity insertion.

Wetting angle can be affected by changes in Flibe chemistry and the graphite material properties. Flibe properties are described in the topical report "Reactor Coolant for the Kairos Power Fluoride Salt-Cooled High Temperature

Reactor" (KP-TR-005). Changes in Flibe chemistry will be slow and the magnitude of change will be maintained within the limits of the specification discussed KP-TR-005. Further, the effect of such changes in chemistry on graphite material properties is on the timescale of years, rather than seconds. Any changes in wetting angle due to Flibe chemistry changes or irradiation damage cannot result in a rapid insertion of positive reactivity.

Neither pressure nor wetting angle can change rapidly enough in the design basis of a KP-FHR to consider reactivity change as a credible safety-significant scenario. The material qualification plan for structural graphite does not include further data collection related to the effect on neutronics of Flibe intrusion into structural graphite in the reactor core.

5.2 ABRASION AND EROSION

Abrasion can cause surface wear, but unless there is a significant dimension reduction caused by abrasion, surface wear on structural graphite will not affect the integrity of ET-10 graphite. The abrasion caused by pebbles sliding against ET-10 is expected to be very low for the following reasons:

1. ET-10 is much harder than the pebble carbon matrix, which is mainly comprised of natural graphite, a softer material
2. Pebbles are buoyant in Flibe so the contact forces between pebbles and the reflector surfaces are very low in comparison with gas-cooled pebble bed reactors

Kairos Power will perform confirmatory tribology testing on pebbles against ET-10 in Flibe to quantify wear rates of ET-10 and to demonstrate that no significant abrasion of the structural graphite occurs due to contact between the reflector and the pebbles. The tribology tests will use sliding speeds, distances, and forces representative of a KP-FHR.

In a system in which materials are chemically compatible, erosion only contributes to surface wear. This is the case for the structural graphite, which is chemically compatible with Flibe (see Section 5.1.3). Therefore, erosion would not affect bulk material properties of the structural graphite. This is supported by the experience in the MSRE experiment in which no erosion was observed for the same grade of graphite in Flibe.

The Division 5 code discussion of erosion is based on factors relevant to a gas cooled reactor and does not specify a need for testing. The Division 5 Code states that in a gas cooled reactor erosion should be evaluated if the gas flow velocity is greater than 100 m/s, when considering oxidation. Flibe velocity in a KP-FHR will be 1-2 orders of magnitude below 100 m/s. Erosion of the structural graphite will be captured in the Flibe corrosion tests using the Rotating Cage Loop (RCL) Test System in Flibe. This test system is designed to measure Flibe corrosion of stainless steel, but the system also includes ET-10 graphite to be representative of the Kairos Power reactor vessel corrosion conditions. During operation, the RCL sample cage rotates in Flibe at 500 RPM with a surface velocity of 3.4 m/s and is separated from a stationary ET-10 part by an average of about 15mm. The duration of RCL tests will be in excess of 3,000 hours. Wear on the graphite blocks in the reflector due to erosion would be less than those from the abrasion of pebbles on the reflector blocks. Therefore, the effects of abrasion due to pebbles is expected to bound the effects of erosion from Flibe. Kairos Power will confirm through visual inspection of ET-10 in the RCL tests that no significant loss of volume will occur in the structural graphite due to erosion.

5.3 OXIDATION OF GRAPHITE

In a KP-FHR, most of the structural graphite components are immersed in Flibe molten salt. The top reflector above the molten salt is protected by the Argon cover gas, as discussed in Section 1.1.3. The density of Argon gas is ~25% higher than that of oxygen (Ar, 0.492 kg/m^3, O_2, 0.393 kg/m^3, at 700°C, 1 bar). In normal operating conditions, Ar gas naturally acts as a protection layer above the top reflector in the event that trace amounts of air enters the Ar gas. Therefore, oxidation in normal operating conditions is not expected.

In the event that air leaks into the cover gas, oxidation may occur at the top of the reflector that is not immersed in Flibe molten salt. In addition, oxidation may also occur in the graphite reflector materials that are immersed in Flibe. [[

]].

The main concern with the graphite oxidation is a potential loss of the strength. Kairos Power will conduct a design-specific analysis to demonstrate that the weight loss due to oxidation does not challenge a design limit for the reflector structure. The results of the analysis would be provided in an application for an operating license.

The assessment of the effect of oxidation on graphite strength will be conducted separately in the safety analysis program. For exposed graphite not submerged in Flibe, this involves two major tasks: (1) determine the weight loss of graphite under the postulated event conditions; (2) determine the strength reduction due to the oxidation. The steps to accomplish these tasks are highlighted below.

1. Determine basic oxidation characteristics of ET-10, e.g., rate of oxidation per ASTM D7542.
2. Determine the effective gas diffusivity of ET-10.
3. The parameters obtained from Task #1 and #2 will be fed into a newly developed model by INL to generate the oxidation depth profile and weight-loss profile.
4. As confirmation and model validation, the weight loss value will be obtained experimentally. The oxidation temperature and duration will bound the conditions determined by the safety analysis. Kairos Power's early estimate is that testing will start by using a temperature of 750°C and a duration of 3 days. The safety analysis scenario definition will account for cover gas supply.
5. Determine strength reduction based on the relationship between strength and weight-loss, which will be established for ET-10 grade graphite through the testing program. The planned temperature range is 550 – 750°C (Kinetic regime).

For the assessment of graphite submerged in Flibe, where there is air ingress in the cover gas under postulated event conditions, the two major tasks are: (1) determine if there is oxidation by observing porosity or density change; (2) if there is significant oxidation by porosity or density change, as compared to air oxidation experiments, then determine the strength reduction due to the oxidation. The steps to accomplish these tasks are highlighted below.

1. Determine the changes in porosity or density due to oxidation of graphite submerged in Flibe.
2. If oxidation is significant, then demonstrate the structural integrity bounds the effects of oxidation.

To assess the structural integrity of the top reflector due to the oxidation, stress levels experienced by the top reflector blocks will be compared to the material's strength values and, if applicable, relevant ASME allowable stress limits. The elastic modulus of unoxidized graphite will be used to predict internal stresses. This is conservative

because the elastic modulus will decrease due to the oxidation, which means that using the elastic modulus value corresponding to unoxidized graphite will lead to higher predicted stress levels in modeling.

Thermal conductivity will also decrease as a result of oxidation. However, KP-FHR does not rely on the top reflector for heat dissipation (to cover gas). The design is based on an adiabatic thermal boundary condition between top reflector and cover gas, where oxidation may occur in the event of air ingress. Therefore, the decrease of thermal conductivity of graphite at the top reflector is not a factor impacting its safety function. Thermal conductivity is not expected to be significantly affected due to oxidation in the submerged graphite. Kairos Power will not measure the thermal conductivity of the oxidized graphite in the qualification program.

In summary, for normal operation, oxidation is not expected for the structural graphite ET-10 because the material is in an inert environment. This can be confirmed in future license applications which will contain design details for the Cover Gas System. In postulated event conditions safety analysis will characterize the potential and quantity of air ingress. Testing will quantify the reduction in strength in postulated event conditions for the reflector based on the inputs from the safety analysis and the data from INL correlating graphite strength change with weight loss.

6 SEISMIC RESPONSE

Seismic response is a consideration in the design of the structural graphite in the reflector. Seismic response of the KP-FHR reflector structure differs from MHTGRs because the structure is positively buoyant and the incompressible Flibe in gaps between reflector blocks provides substantial damping, greatly reducing mechanical loads. The seismic qualification plan for the structural graphite is outside the scope of this report and will be addressed in a separate submittal supporting a licensing application.

7 CONCLUSIONS AND LIMITATIONS

7.1 CONCLUSIONS

Kairos Power has selected ET-10 graphite grade for use in safety-related structural graphite component design. This report presents the qualification plan for that material for use in a KP-FHR. The qualification plan for unirradiated and irradiated graphite conforms with the Division 5 code with limited departures.

The qualification program includes qualification testing to measure thermal and mechanical properties of as-manufactured ET-10 at room temperature, which provides conservative values for subsequent modeling for use in structural analysis. Existing irradiation data will be leveraged and no irradiation creep data on ET-10 will be collected to support a graphite reflector 4-year component lifetime (i.e., pre-turnaround). An irradiation test will be performed to measure the irradiation creep properties of ET-10 under irradiation for longer graphite reflector component lifetimes (past-turnaround). This report describes the testing plans that will be used to provide that irradiation creep property data.

Literature data exists to demonstrate the compatibility of structural graphite with Flibe for most environmental compatibility phenomena. This qualification plan also includes a few limited phenomena for which Kairos Power proposes to conduct additional testing to demonstrate compatibility of structural graphite in a Flibe environment.

Seismic qualification of structural graphite components is outside the scope of this report and will be addressed as part of subsequent licensing applications.

7.2 LIMITATIONS

This report is limited to the qualification of structural graphite materials for safety-related, high temperature components in the KP-FHR. Kairos Power is requesting Nuclear Regulatory Commission review and approval of the qualification plan described in this report for use by licensing applicants under 10 CFR 50 or 10 CFR 52.

The conclusions in this report are based on the following considerations:

- Flibe infiltration is not a consideration for the KP-FHR when limited to reactor vessel fluid heights up to 4 m.
- Additional irradiation creep data from testing of ETU-10 is not required when the turnaround fluence is greater than the component lifetime.
- Graphite qualification presumes the reflector does not undergo freeze-thaw cycles if Flibe has infiltrated the graphite structure.
- The primary coolant loop for a KP-FHR power reactor will be at a higher pressure than an interfacing system that uses a different intermediate salt than the primary salt during both normal operation and postulated event conditions. This precludes by design the infiltration of intermediate salt into the reactor vessel in which the structural graphite is housed. A future license application will evaluate and justify the effects of unplanned intermediate salt infiltration into the primary loop, if the reactor design uses intermediate salt in an interfacing heat transfer loop.
- The reflector structure and reactor vessel design preclude the coincident effects of oxidation and irradiation such that the structural integrity of the top of the reflector would be unable to perform its safety function. This will be discussed in a future license application that relies on the qualification program described in this report.

- **A future license application will demonstrate that ET-10 unirradiated fatigue response follows the same trends as H-451 and PGX.**
- **A future license application that relies on the qualification program in this report will demonstrate that the data relied on for qualification bounds the analysis for irradiated properties.**
- **A design specific analysis of the effect of weight loss due to graphite block oxidation on structural integrity of the reflector material will be provided in a future license application that references the qualification program described in this report.**

8 REFERENCES

1. ASME, *Rules for Construction of Nuclear Power Plant Components, High Temperature Reactors*, Boiler and Pressure Vessel Code, Section III, Division 5. 2017 Edition

2. University of California Berkeley Nuclear Engineering. 2015. *Fluoride Salt Cooled High Temperature Reactor*. [ONLINE] Available at:http://fhr.nuc.berkeley.edu. (Accessed 20 December 2020).

3. Kairos Power, LLC, *Design Overview of the Kairos Power Fluoride Salt Cooled, High Temperature Reactor*. KP-TR-001, Revision 1. February 2020.

4. Kairos Power, LLC, *Metallic Materials Qualification for the Kairos Power Fluoride Salt-Cooled High-Temperature Reactor*, KP-TR-013-P, Revision 0. June 2020.

5. Kairos Power, LLC, *Principal Design Criteria for the Kairos Power Fluoride Salt Cooled High Temperature Reactor*, KP-TR-003-P-A. May 2020.

6. Burchell, T., Bratton, R., and Windes, W., *NGNP Graphite Selection and Acquistion Strategy*. ORNL/TM2007/153. 2007.

7. Burchell, T.D., *Radiation Effects in Graphite*, Comprehensive Nuclear Materials, Vol. 4, pp.299-324. 2012.

8. W. Windes, *Irradiated Graphite Data and Analysis*, ART Gas-Cooled Reactor Program Review. 2020.

9. ORNL, *Report on Effects of Irradiation on Material ETU-10*. ORNL/TM-2017/737. 2017.

10. Rosenthal, M. W., *The Development Status of Molten-Salt Breeder Reactors*, ORNL-TM-4812. 1972.

11. NRC, *Phenomenon Identification and Ranking Tables (PIRTs) for Loss-of-Coolant Accidents in Pressurized and Boiling Water Reactors Containing High Burnup Fuel.* NUREG/CR-6944, Vol. 5. March 2008.

12. INL, *Graphite Technology Development Plan*, INL/EXT-07-13165. September 2007.

13. ORNL, *Technical Gap Assessment for Materials and Component Integrity Issues for Molten Salt Reactors*, ORNL/SPR-2019/1089. March 2019

14. Georgia Institute of Technology, *Phenomena Identification and Ranking Tables (PIRTs) Report for Material Selection and Possible Material Degradation Mechanisms in FHR*, April 2017

15. SGL Carbon, *SIGRAFINE ISO graphite for electronic applications*, [online] Available at: https://www.sglcarbon.com/pdf/SGL-TDS-SIGRAFINE-ISO-for-Electronic-Applications-EN.pdf

16. Price, R.J., *Cyclic Fatigue of Near-Isotropic Graphite: Influence of Stress Cycle and Neutron Irradiation*, Carbon, Vol. 16, pp. 367-372. 1977.

17. JAERI-Research 98-024, "The fatigue strength of graphite and carbon materials for HTTR core components", 1998.

18. ASME BPV Code, Section III, Division 5, HHA-III-5000, *Use of Historical Data*. 2017.

19. ORNL/TM-2014/86, Graphite Post-Irradiation Testing Program – Test Specification – Ibiden Japan. 2014.

20. Price, R J., *Strength of Irradiated Graphite: A Revie,*. Specialists Meeting on Mechanical Behaviour of Graphite for HTRs, no. July: 69–76. 1979.

21. Ishiyama, S., Burchell, T. D., Strizak, J. P., and Eto, M., *The Effect of High Fluence Neutron Irradiation on the Properties of a Fine-Grained Isotropic Nuclear Graphite.* Journal of Nuclear Materials 230 (1): 1–7. 1996.

22. Ball, D., *Graphite for High Temperature Gas-Cooled Nuclear Reactors*, STP-NU-009. 2008.

23. Davies, M. A., Bradford, M., *A Revised Description of Graphite Irradiation Induced Creep*. Journal of Nuclear Materials, 381(1–2), 39–45. 2008.

24. Price, R. J., *Irradiation-Induced Creep in Graphite: A Review*. 1981.

25. Marsden, B. J., Haverty, M., Bodel, W., Hall, G. N., Jones, A. N., Mummery, P. M., Treifi, M., *Dimensional Change, Irradiation Creep and Thermal/Mechanical Property Changes in Nuclear Graphite*, International Materials Reviews, 61(3), 155–182. 2016.

26. Oku, T.; Eto, M., Ishiyama, S., *Irradiation Creep Properties and Strength of A Fine-Grained Isotropic Graphite*. Journal of Nuclear Materials, 1, 77–84. 1990.

27. Mobasheran, A. S., PhD thesis, University of Tennessee, USA. 1990.

28. Haag, G., *Properties of ART-2E Graphite and Property Changes due to Fast Neutron Irradiation*, Reports From the Research Center in Jülich, Germany. 2005

29. Brocklehurst, J., Kelly, B., *A Review of Irradiation Induced Creep in Graphite Under CAGR Conditions*, UKAEA Report ND-R-1406 (S). June 1989.

30. Windes, W. E., Rohrbaugh, D. T., Swank, W. D., *AGC-3 Irradiation Creep Strain Data Analysis,* (INL/EXT-19-54725). July 2019.

31. Gray, W. J., *Constant Stress Irradiation-Induced Compressive Creep of Graphite at High Fluences*, Carbon, 11(4), 383–392. 1973.

32. Burchell, T., *Irradiation Induced Creep Behaviour of H-451 Graphite*, Journal of Nuclear Materials, 381, 46-54. 2008.

33. Gray, B., Brocklehurst, J., *The Irradiation-Induced Plasticity in Graphite Under Constant Stress*, United Kingdom Atomic Energy Authority, TRG Report 1071 (C). 1966.

34. Kelly, B. T., & Brocklehurst, J. E., *UKAEA Reactor Group Studies of Irradiation-Induced Creep in Graphite*. Journal of Nuclear Materials, 65(C), 79–85. 1977.

35. Kairos Power, LLC, *KP-FHR Fuel Performance Methodology*, KP-TR-010, Revision 2. November 2020.

36. Kreyger, P. J., Kirslis, S. S., Blankenship, F. F., *Reactor Chemistry Divison Annual Progress Report*, ORNL-3591. 1964.

37. Washburn, E. W.; *Note on a Method of Determining the Distribution of Pore Sizes in a Porous Material,* Proc. Natl. Acad. Sci., vol. 7, p. 115. April 1921.

38. Sohal, M.; Ebner, M.; Sabharwall, P.; *Engineering Database of Liquid Salt Thermophysical and Thermochemical Properties*, INL/EXT-10-18297. 2010.

39. Xu, H. X.; Lin, J.; Zhong, Y. J., *Characterization of molten 2LiF-BeF$_2$ salt impregnated into graphite matrix of fuel elements for thorium molten salt reactor*. Nucl Sci Tech. 2019.

40. Gallego, N., Contescu, C., and Keiser, J., *Progress report on graphite-salt intrusion studies TM-2020/1621*, ORNL. 2020.

41. Zhang, C.; Tang, H.; He, Z.; *Dataset on the Mechanical Property of Graphite After Molten FLiNaK Salt Infiltration*, Data in Brief, Vol. 21, pp. 1963-1969. 2018.

42. Zhang, C.; He, Z.; Gao, Y.; et. al; *The Effect of Molten FLiNaK Salt Infiltration on the Strength of Graphite*, Journal of Nuclear Materials, Vol. 512, pp. 37-45. 2018.

43. Qi, W.; He, Z.; Tang, H.; *Effects of FLiNak infiltration on thermal expansion behavior of graphite*, Journal of Material Science, Vol. 52, pp. 4621-4634. 2017.

44. He, Z.; Gao, L.; X. Wang, X.; *Improvement of Stacking Order Ingraphite by Molten Fluoride Salt Infiltration*, Carbon, Vol. 72, pp. 304-311. 2014.

45. Shiel, R. J.; Evans, R. B.;Watson, G. M.; *Molten Salt-Graphite Compatibility Test*, ORNL-59-8-133. 1959.

46. ORNL, *Postirradiation Examination of Materials from the MSRE*, ORNL-TM-4174, 1972.

47. Yang, X.; Feng, S.; Zhou, X.; *Interaction Between Nuclear Graphite and Molten Fluoride Salts: A Synchrotron Radiation Study of the Substitution of Graphite Hydrogen by Fluoride Ion,* Journal of Physical Chememistry, Vol. 116, No. 3, pp. 985-998. 2012.

48. Wu, H.; Carotti, F.; Gakhar, R.; *Fluorination of Nuclear Graphite IG-110 in Molten 2LiF-BeF2 (FLiBe) Salt at 700°C*, Journal of Fluorine Chemistry, Vol. 211, pp. 159-170. 2018.

49. Lewis, I. C.; *Chemistry of Carbonization*, Carbon, 1982, Vol. 20, Issue 6. 1982.

50. Bernardet, V.; Gomes S.; Delpeux, S.; *Protection of Nuclear Graphite Toward Fluoride Molten Salt by Glassy Carbon Deposit,*" Journal of Nuclear Materials, Vol. 384, pp. 292-302. 2009.

51. Nakajima, T.; Kasayuki, M.; Watanabe, N.; *Graphite Intercalation Compound of Fluorine with Lithium Fluoride*, Synthetic Metals, Vol. 7, No. 1-2, pp. 117-124. 1983.

52. He, Z.; Tang, H.; Gao, L.; *Graphite and Molten Salt Compatibility Evaluation*, 15th International Nuclear Graphite Specialist Meeting, Hangzhow, China. 2014

53. Sturm, B. J.; Blankenship, F. F.; Reactor Chemistry Division Annual Progress Report, ORNL-2391. 1960.

54. Olson, L.C. Ambrosek, J.W., Sridharan, K., Anderson, M.H., Allen, T.R., *Materials Corrosion in Molten LiF-NaF-KF Salt*, Journal of Fluorine Chemistry, 130, 67-73. 2009.

55. Sumita, J., *Evaluation of Fracture Toughness of Fine and Coarse-Grain Graphite*, 14th INGSM, Seattle, USA. 2013.

56. Burchell, T., Erdmann, D., and Hunter, J., *The Fracture Toughness of Nuclear Graphite Grades, TM-2016/678*, ORNL. 2017.

57. Toyo Tanso, manufacturer data, [ONLINE] Available at: https://www.toyotanso.com/Products/Special_graphite/data.html, (Accessed 21 December 2020)

58. Ibiden, manufacturer data, [ONLINE] Available at: https://www.fgm.ibiden.co.jp/multilanguage/english/list.html, (Accessed 21 December 2020), (Accessed 21 December 2020)

59. Campbell, A., and Katoh, Y., *Summary Report on Effects of Irradiation on Material IG-110, TM-2018/1040*, ORNL. 2018.

60. Snead, M., Katoh, Y., and McAlister, M., *Graphite Pre-Irradiation Specimen Size Validation and Testing Program Ibiden Japan results.* TM-2013/229, ORNL, 2013.

61. He, Z.; Tang, H.; *Molten-Salt-Infiltration/Diffusion in Graphite and Microcrack Characterization Using SAXS*, 17th International Nuclear Graphite Specialist Meeting, Vienna, Austria. 2016.

62. Cathcart, H. A., et al., *Validation of Dimensional Change Modelling Through Outage Expectations*, 6th EDF Energy Nuclear Graphite Conference, Kendal, UK. October 2018.

63. Kelly, B. T,. *The Effect of Substitutional Boron on Irradiation Damage in Highly Oriented Pyrolytic Graphite Irradiated at 60°,*. Carbon 16 (6): 499–501. 1978.

64. Schofield, P., Daniels, P. R. C., Brocklehurst, J. E., and Harper, A., *Graphite Fast Neutron Damage/Radiolytic Oxidation Interaction Experiment: Final Report*. AEA TRS 5054,CSDMC/P38/1. 1990.

65. Not used.

66. Not used.

67. Skipper, S., Perktold, J., "*Statsmodels: Econometric and statistical modelling with Python,* Proceedings of the 9th Python in Science Conference. 2010.

68. Salvatier, J., Wiecki, T. V., Fonnesbeck, C., *Probabilistic programming in Python using PyMC3,* PeerJ Computer Science 2. 2016.

69. Campbell, Anne A., *Cumulative Results of Irradiation Induced Creep of Material IG-110 - Prepared for Toyo Tanso Co ., Ltd*. 2018.

70. van Staveren, T. O., Davies, M. A., Knol, S., and de Koning, A. J., *Design, Construction and Operation of a Graphite Irradiation Creep Facility*, Nuclear Engineering and Design, 364 (April): 110588. 2020.

Table 1. Summary of Key Parameters for the KP-FHR

Parameter	Value/Description
Reactor Type	Fluoride-salt cooled, high temperature reactor, pool-type
Core Configuration	Pebble bed core, graphite moderator/reflector, and enriched Flibe molten salt coolant
Physical Dimensions	Reactor Vessel is up to ~4 m diameter, 6 m height
Reactor Thermal Power	~320 MW_{th} (power reactor), up to 35 MW_{th} (non-power reactor)
Reactor Coolant and Operating Range	Flibe Salt, 550°C - 650°C
Material for Safety-Related Structures	ASME Section III, Division 5, ET-10, 316H, ER16-8-2

Table 2. Graphite Properties, Characteristics and Performance Attributes

Properties	Requirement and characteristics	Attributes
Bulk density	Typically requires greater than 1.7g/cm^3 to be effective for neutron moderation/reflection per unit volume. Higher density is indicative of higher strength for the similar grades.	Neutron efficiency and structural integrity
Strength and modulus	Adequate strength is required for structure component integrity. Typical requirement for extruded and molded graphite, ≥ 15 MPa (tensile strength in WG); Isomolded graphite, ≥ 22 MPa (tensile strength in WG). Dynamic Elastic modulus, 8-15 GPa (WG) for all the grades. The strength must exceed allowable operating component stresses. Higher strength material has higher modulus, normally lower fracture toughness. The trade-off between strength and modulus must be taken into account in graphite selection. Strength and modulus are temperature dependent, increase with temperature.	Structural integrity
Coefficient of Thermal Expansion (CTE)	CTE is mainly determined by coke CTE. Typical nuclear graphite CTE is 3.5-5.5x10^{-6}/°C (WG, 25-500°C). The anisotropy ratio is defined as CTE ratio, CTE_{AG}/CTE_{WG}. The typical value for isotropic graphite is 1.00 to 1.10; near-isotropic graphite is 1.10 to 1.15. Isotropic coke produces graphite with higher CTE but is more isotropic (lower anisotropy ratio), which has better dimensional stability. However, lower CTE is beneficial in terms of thermal stress. CTE is temperature dependent, increases with temperature.	Structure integrity
Thermal conductivity	Thermal conductivity is mainly determined by the graphitization temperature and coke type. Typical nuclear graphite requires thermal conductivity (W/m·K, AG at 25°C): ≥ 100 for extruded and molded graphite, ≥90 for isomolded graphite. Higher thermal conductivity is more efficient for heat transfer in the reactor. Thermal conductivity is also temperature dependent, decreases with temperature.	Heat transport
Purity	Equivalent Boron Content, EBC, is a key purity specification for nuclear graphite. The requirement for a gas cooled reactor is ≤2 ppm for high purity graphite and ≤10 ppm for low purity graphite. Ash ≤ 300 ppm, for low neutron irradiation dose application, to minimize impurity acting as oxidation catalyst.	Neutron efficiency and oxidation rate

Table 3. Structural Graphite Material (ET-10 and ETU-10) Property Data

[[

]]

Table 4. Proposed Research Areas Identified by INL and the Structural Graphite Material Qualification Plan Elements

Topic	Impact	Relation to KP-FHR Material Qualification Plan
Structural integrity of graphite	Retention of long-term structural stability and mechanical strength under specified loads. Specified by ASME requirements.	Addressed by ASME Section III, Division 5 requirements. See Sections 3, 4, and 5 of this report.
Thermal response of graphite – normal operation	Changes in thermal properties at peak dose and temperatures.	Changes in ETU-10 thermal properties under irradiation are known (see Section 5)
Thermal response of graphite – off-normal operation	Verification that changes to thermal material properties is sufficiently small to guarantee the passively safe response of the reactor.	Qualification data generated under the structural graphite material qualification plan will be used in subsequent modeling to predict thermal response.
Changes to by-pass flow	Potential coolant flow issues due to shrinkage and swelling of graphite components.	Qualification data generated under the structural graphite material qualification plan will be used in subsequent modeling of by-pass flow.
Chemical and mechanical core stability	Oxidation and subsequent structural stability of oxidized graphite. For both acute (postulated event) and chronic (normal operation) conditions.	No oxidation in KP-FHR. (See Section 5.2)

Table 5. Applicable ASME and ASTM Code for Structural Graphite Material Qualification

Property to be Qualified	ASME Section III, Division 5 Code and related ASTM Standard
Mechanical and Thermal Properties	HHA-II-2000, Material Data Sheet, Form MDS-1 HHA-III-3100, As-manufactured graphite HHA-III-4000, Requirement for representative data ASTM C781 Standard Practice for Testing Graphite Materials for Gas-Cooled Nuclear Reactor Components ASTM D7775 Standard Guide for Measurements on Small Graphite Specimens
Property Variation	HHA-III-5000, Use of historical data
Purity	ASTM D7219-08, Standard specification for isotropic and near-isotropic nuclear graphite materials ASTM C1233-15 Standard practice for determining equivalent Boron contents for nuclear materials
Molten Salt Infiltration	ASTM D8091 Standard Guide for Impregnation of Graphite with Molten Salt
Oxidation	ASTM D7542 Standard Test Method for Air Oxidation of Carbon and Graphite in the Kinetic Regime HHA-III-3200 Oxidized graphite

Table 6. Test Matrix for Graphite Physical Properties

[[

]]

Table 7. ASTM International Standard and Specimen Dimensional Requirements

Property	ASTM standard	Specimen dimensional requirement
Bulk density	C559	ø10x60 mm, at room temperature
Flexural strength	C651	2.5x5x60 mm
Tensile strength	C749	ø12.95x120.65 mm, center section ø6.35 mm
Compressive strength	C695	ø6x12 mm (tentative) (If Kairos Power decides to use this sub-sized sample, smaller than ASTM C695 recommended size(ø9.5x19 mm), the effect of sample size will be studied per the guidance in ASTM D7775 Standard Guide for Measurements on Small Graphite Specimens.
Dynamic YM and Shear Moduli	C747	2x10x50 mm
Coefficient of Thermal Conductivity	E228	ø10x60 mm
Thermal Conductivity	E1461	ø10x2 mm

Table 8. Trace Element Analysis of ET-10 by Glow Discharge Mass Spectrometry

[[

]]

Table 9. Available Basic Properties Data for ETU-10

Source	Irradiation temperature	Fast fluence range	Properties measured
ORNL, *Report on Effects of Irradiation on Material ETU-10*. (ORNL/TM-2017/737)	300°C to 740°C (dimensional change) / 695°C (other properties)	Depends on irradiation temperature	Dimensional change CTE Thermal conductivity Young's Modulus Strength

Reference 9

Table 10. Irradiation Creep Test Matrix for ET-10 in a Power KP-FHR

[[

]]

Table 11. Summary of Historical Experimental Conditions for Irradiation Creep Data Compilation

Experiment/Reference	Graphite Grades	Maximum Dose (dpa)	Estimated Temperatures (°C)	Stresses (MPa)	Compressive or Tensile
Haag	ATR-2E	28.0	300, 500, 550	5.0	Both
OC	H-327, H-451	3.6	600, 900	13.8, 20.7	Compressive
Oku	IG-110	2.0	750 to 1000	9.0 to 13.5	Compressive
PLUTO	IM1-24, VNMC, SM2-24	3.0	850, 1050	5.5, 11.0, 22.1, 44.2	Compressive
AGC	Various	7.0	600, 800	13.8, 20.7	Compressive
Gray	AGOT, H-337, AXF-8QBGI	10.5	550, 800	7 to 21	Compressive
Burchell	H-451	13.6	900	6.0	Tensile
BR2	PGA, Various Isotropic	7.5	300 to 650	6.0	Both

Table 12. Summary of Graphite Grades Analyzed for Irradiation Creep Data Compilation.

Grade	Type	Manufacture Process
2114	Non-petroleum coke, fine grain, isotropic	Isostatically pressed
AGOT	Needle coke	Extruded
ATR-2E	Medium grain, pitch coke graphite, near-isotropic	Extruded
AXF-8Q	Fine grain, isotropic	Isostatically molded
H-327	Needle coke	Extruded
H-337	Near-isotropic	Extruded
H-451	Medium grain, near-isotropic	Extruded
IG-110	Fine grain, isotropic	Iso-molded
IG-430	Fine grain, isotropic	Isostatically pressed
IM1-24	Gilsocarbon	Molded
NBG-17	Medium grain, coal coke	Vibrational molded
NBG-18	Medium grain, coal coke	Vibrational molded
PCEA	Petroleum coke	Extruded
SM2-24	Petroleum coke	Molded
VNMC	Coal tar pitch coke	Molded

Table 13. Physical Properties of ETU-10 and IG-110

Property	**ETU-10**	**IG-110**
Classification, coke type	Superfine isomolded, pitch coke	Superfine isomolded, Pet coke
Grain size (Max/Average), µm	40/15	50/20
Bulk density, g/cm^3	1.75	1.77
Flexural strength, MPa	58.8(3-points)	39
Tensile strength, MPa	34.3	25
Compressive strength, MPa	98.0	78
Young's modulus, GPa	10.8	9.8
Coefficient of thermal expansion, $x10^{-6}/°C$	3.8	4.5
Thermal conductivity, W·m/K	104.4	120
Fracture toughness, K_{IC}, $MPa*m^{1/2}$	0.93[a]	0.87[b], 1.07[c]

[a] Reference 55
[b] Reference 55
[c] Reference 56

Source: manufacturer's websites (References 57 and 58), unless otherwise noted. The ETU-10 data is identified as ET-10 on the Ibiden website. The IG-110 data is identified as IG-11 on the Toyo Tanso website.

Table 14. Flibe infiltration test matrix

[[

]]

Table 15. Text matrix of effect of Flibe infiltration on ETU-10's strength

[[

]]

Table 16. Summary of literature results on fluorination and its potential impact to graphite structure

	Fluorination through hydrocarbon and oxygen functional structure, (Reference 47 and 48)	**Fluorination on defects in graphite edge plane** (Reference 48)	**Fluorination through Intercalation** (References 48, 50, and 51)
Is massive fluorination at bulk level possible?	No	No	Yes.
Is structure degradation possible?	No	No evidence reported	Yes. Through exfoliation
Comments on literature results	Hydrocarbon and oxygen functional structure are thermally unstable. Trace amount in graphite, if any. Majority fluorination observed is this type.	This type is limited by the available defects in graphite, could compete with Tritium adsorption on the defects.	Confirmed by XRD, no intercalation occurs.

Table 17. Comparison of IG-110 and ETU-10 Properties Measured by ORNL with Similar Specimen Size

Property	IG-110[a]			ETU-10[b]		
	Specimen size, mm	Orientation	Average (std. dev.)	Specimen size, mm	Orientation	Average (std. dev.)
Bulk density	all	both	1.77 (0.017)	all	both	1.759 (0.020)
Dynamic YM, GPa	25x3x2.9	AG	9.1 (0.23)	24x5x1	AG	8.67(0.14)
		WG	9.7 (0.22)		WG	10.14(0.24)
Flexural strength, 4-pts, MPa	25x3x2.9	AG	34 (1.8)	45x4x3	AG	53.47(1.92)
		WG	36 (1.3)		WG	60.33(2.00)
Coefficient of Thermal Expansion 25-500°C, $x10^{-6}$/°C	25x3x2.9	AG	4.5 (0.04)	30x3x2.5	AG	4.15 (0.03)
		WG	4.2 (0.11)		WG	3.74 (0.02)
Anisotropy ratio	-	-	1.06	-	-	1.11
Thermal conductivity @25°C, W/m·K	ø6x4	AG	129(7.2)	ø6x4	AG	82.79 (2.29)
		WG	130(3.7)		WG	88.69 (3.08)
Thermal conductivity @500°C, W/m·K	ø6x4	AG	73 (3.5)	ø6x4	AG	n/a
		WG	77 (1.4)		WG	70.52 (2.91)

[a] Reference 55
[b] Reference 60

Note: original data format from the ORNL reports is preserved

Table 18. Comparison of Pore Structure Parameters

Graphite grade	Bulk density[a,b] (g/cm^3)	Skeletal density[a] (g/cm^3)	Open porosity (%)	Closed porosity (%)	Total porosity[c] (%)	Entrance pore diameter[a,d] (μm)	Hg intrusion volume[a,d] (cm^3/g)
IG-110	1.76	2.05	14.2	7.2	21.4	3.9	0.06
ETU-10	1.74	2.10	17.1	5.2	22.3	3.6	0.09

[a] ORNL data (Reference 40)
[b] value from the corresponding specimen for skeletal density and Hg porosimetry measurement
[c] calculated based on graphite theoretical density of 2.24g/cm^3
[d] from Hg porosimetry measurement.

Table data comes from Reference 40, with footnotes indicating the type of information or its calculation basis.

Figure 1. Overview of a KP-FHR Heat Transport Loops with Nominal Operating Temperatures

[[

]]

Figure 2. Steps in the Manufacture of Synthetic Graphite

[[

]]

Figure 3. Illustration of the Effects of Irradiation Temperature on Turnaround Rates

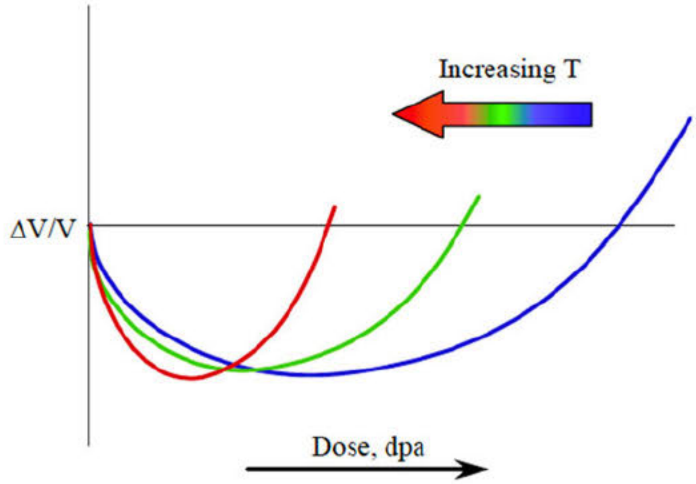

Reference 12

Figure 4. Temperature Dependent Properties of ET-10 from Ibiden: Flexural Strength

[[

]]

Figure 5. Temperature Dependent Properties of ET-10 from Ibiden: Elastic Modulus

[[

]]

Figure 6. Temperature Dependent Properties of ET-10 from Ibiden: Coefficient of Thermal Expansion

[[

]]

Figure 7. Temperature Dependent Properties of ET-10 from Ibiden: Thermal Conductivity

[[

]]

Figure 8. Sample Graphite Specimen Cutting Pattern

[[

]]

Figure 9. Example of Graphite Sample Cutting Plan for Local Variation Analysis (Billet Uniformity)

[[

]]

Figure 10. Local strength variation of ET-10

[[

]]

Figure 11. Example of Density Variation of ET-10

[[

]]

Figure 12. Representative Temperature and Fast Neutron Flux Distributions in the Graphite Reflector

[[

]]

Figure 13. Point Cloud of Irradiation Conditions for Which ETU-10 Basic Properties Were Characterized by ORNL

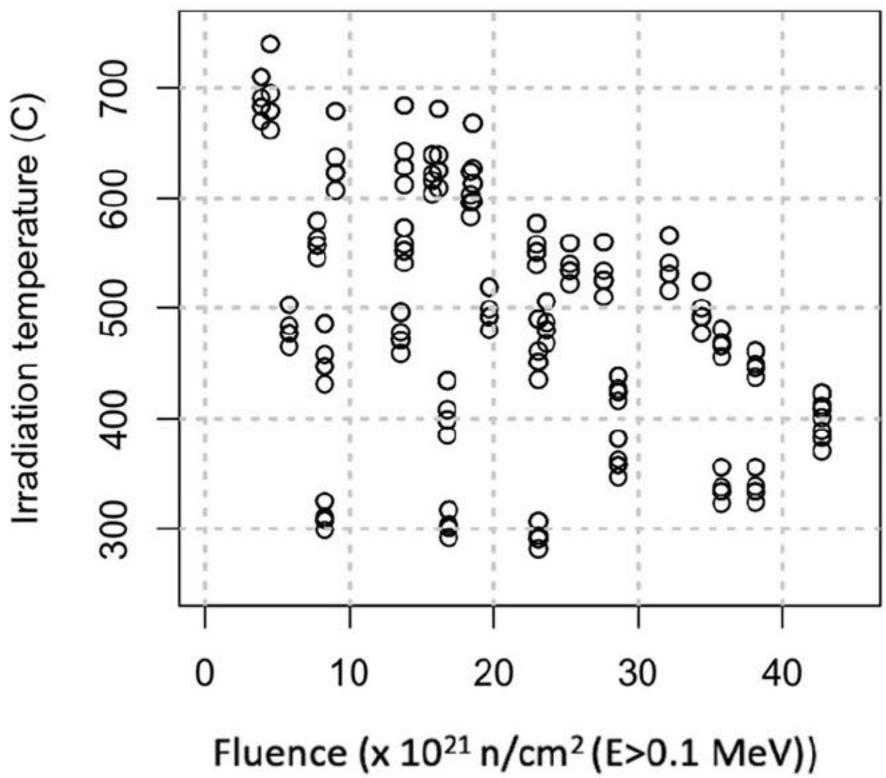

Reference 9

Figure 14. Irradiation Temperature-Fluence Envelope for ETU-10

[[

]]

Figure 15. Convex Hull Envelope for the ORNL Dimensional Change Data

[[

]]

Figure 16. Calculated Secondary Creep Coefficients Plotted Against Irradiated Temperature

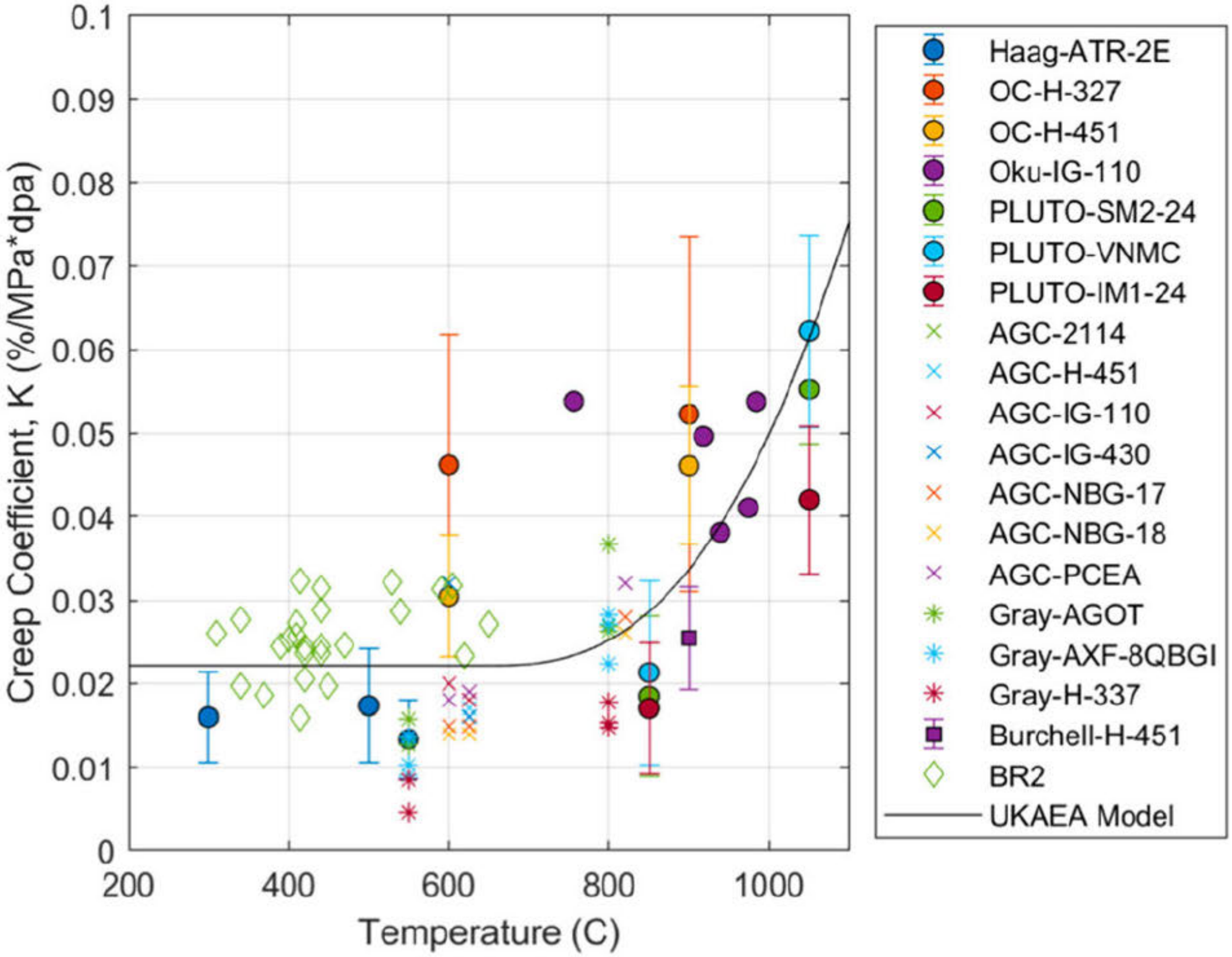

Error bars represent experiments where data is available over dose ranges and show the mean creep coefficient and +/-1σ of the sample measurements. The UKAEA creep model is also shown for reference (Reference 34).

Figure 17. Relationship Between Flibe Infiltration Threshold Pressure and Entrance Pore Diameter

[[

]]

Figure 18. Illustration of Pressure and Temperature Gradients in a Power KP-FHR

[[

]]

Figure 19. Effect of Infiltrated Salt on Mechanical Strength at 700°C

[[

]]

Figure 20. Thermal Expansion of Graphite With and Without FLiNaK Infiltration

[[

]]

Figure 21. Temperature profile and oxidation duration in the postulated event (the thin line)

[[

]]

APPENDIX A. Data Analysis

Many testing programs that are expected to yield quantitative results were developed with the intent of statistical analysis of the data. These data will be analyzed via standard statistical methods. For those data generated to support the material qualification plan for structural graphite, Kairos Power will establish the material properties of the structural graphite. Kairos Power will also use those data to establish irradiated graphite basic properties and irradiation creep data. The creep data will be used in irradiation creep models. The irradiation creep model will utilize appropriate prediction bands to ensure appropriate and conservative extrapolation from test conditions to KP-FHR operational times and conditions.

Analysis of mechanical properties (i.e., strength) will follow guidance given in the Division 5 Code, article HHA-II-3100, Material Reliability Curve Parameters (See Section 3).

APPENDIX B. ETU-10 Demonstration of Historical Data Applicability

The Division 5 code provides in HHA-III-5000 that a qualification program for structural graphite may rely on historical data if it can be demonstrated that the historical data was generated using the same grade of graphite. For the purposes of this material qualification, Kairos Power considers a graphite grade from different production lots to be "the same" if they meet the definition of a grade of graphite provided in ASME Code III(5) HAB-9200: "the designation given to a material by a manufacturer such that it is always reproduced from the same raw materials, to the same specifications, using the same process." Based on that definition, the factors that define a grade of graphite and its corresponding material properties are: the raw material, the raw material specification, and the fabrication process. Therefore, Kairos Power considers that two samples of graphite are "the same grade" when the following conditions are met:

<u>Condition 1:</u> The raw material and raw material specification used to manufacture the graphite used in the previous experiments that generated the historical data is the same raw material and specification as would be used to manufacture the structural graphite for a KP-FHR.

<u>Condition 2:</u> The process used to manufacture the graphite used in the previous experiments that generated the historical data is the same process that would be used to manufacture the structural graphite for a KP-FHR.

<u>Condition 3:</u> The as-manufactured properties of the received graphite match the representative values for ET-10 graphite based on historical data from the manufacturer.

ET-10 and ETU-10 are two designations of the same grade of graphite because they are made from the same raw material, the same raw material specification, and the same fabrication process. Also, this is confirmed by data from the manufacturer. See Chapter 3 for more information about ET-10 and ETU-10.

In 2011, ORNL started a series of irradiation tests on ETU-10 graphite (Reference 9). As mentioned in Section 4.3. The range of irradiation temperatures and fluences covered by this ORNL dataset are shown in Figure 14, along with the temperature-dependent turnaround and crossover fluences for ETU-10 as estimated by the same dataset.

The graphite used in the ORNL experiments was ETU-10 manufactured by Ibiden. Ibiden certified that the raw material (pitch coke) and manufacturing process that was used to produce the ETU-10 for the ORNL experiments described in Reference 9, are both the same as will be used to produce the ETU-10 for a KP-FHR. The specifics of the raw material source, raw material specifications, and manufacturing process are intellectual property of Ibiden and are not included in this report. Therefore, based on Ibiden's certification, Conditions 1 and 2 listed in this appendix will be met with respect to verifying that the ORNL dataset was generated using the same grade of graphite. Ibiden will also provide this certification on consistency in raw material and manufacturing process in their material certification report provided with structural graphite manufactured for the KP-FHRs.

With respect to Condition 3 listed in this appendix, Kairos Power will compare the inspection data of each billet ordered with the lot-to-lot variation data as described in Section 3.2.2 of this report to confirm that the graphite properties are consistent. By evaluating the lot-to-lot variation, Kairos Power will meet Condition 3 listed in this appendix.

If the graphite used by KP-FHR meets the three conditions of this appendix, it will be considered the same as the ETU-10 graphite used in the ORNL experiments. Therefore, the dataset developed by ORNL would be applicable to

the graphite that will be used by a KP-FHR. As described in Section 4.3, the dataset developed by ORNL will be relied upon for the qualification of the basic properties of structural graphite in a non-power and a power reactor, and will be relied upon for the data used to establish the turnaround fluence for a non-power reactor.

The ORNL data does not capture all of variability in unirradiated graphite as the specimens are taken from a limited number of billets/locations within billet. Therefore, the irradiated properties models derived from the ORNL data (e.g., Young's modulus as function of fluence) are valid for graphite with the same unirradiated values. For future graphite with different unirradiated values, the ORNL-derived irradiation property models would be scaled to ensure the 0-fluence predictions match the measured unirradiated values. For example, a 10% increase in unirradiated value would lead to scale the irradiation model by 10%. This assumes that unirradiated properties are propagated into irradiated properties, which is justified by the following:

- The ORNL data provides measurement in two grain orientations, and shows that a relative increase in unirradiated values is propagated into the same relative increase in irradiated values
- This scalable behavior is seen in other graphite grade and relied upon by EDF for AGR graphite.

For dimensional change, no unirradiated value is available. Instead, Kairos Power will scale the distribution of the dimensional change model by a factor determined from literature data of billet-billet variation in irradiation-induced dimensional change. For example, such data is available for AGR graphite in Reference 62.

The ORNL data was generated using ETU-10, a.k.a. ET-10 with an additional purification step to remove impurities. After this purification, B is reduced from 0.13 wppm to 0.08 wppm, and Al, Ti, V, Fe are reduced from < 1 wppm to <0.01 wppm levels. This has some benefits on the activity levels of the graphite in the core and for managing graphite during decommissioning. It is known that the dimensional change response of graphite is not affected by B amounts < 35 wppm (References 63 and 64). B-10 absorption cross section for neutron reaction is orders of magnitude larger than the other elements for thermal neutrons and of the same order of magnitude for fast neutrons. As such it is expected that the influence of other elements on graphite irradiation behavior is similar or less than that of B (i.e., they have no influence <1 wppm).

APPENDIX C. Parameter Estimation and Uncertainty Assessment

C.1 OVERVIEW

For a given regression model, e.g., a polynomial functional form, two methods will be used to estimate parameters and explore the uncertainty in parameters when fitting to the ORNL irradiation data. Uncertainty in model parameters will be used to determine uncertainties on turnaround fluences and uncertainty on fit confidence intervals.

1. Ordinary Least-Squares (OLS) regression with bootstrapping uncertainty approach -
   a. An 'uncertainty' is added to each observation to account for measurement uncertainties in irradiation temperature, fluence, and the measured property
   b. New datasets are created by randomly generating 'pseudo' data points normally distributed around the original data with a variance based on the measurement uncertainty
   c. A new model is fitted to each dataset, with a parameter covariance matrix
   d. The family of parameter covariance matrices can be used to calculate uncertainties in model parameters

2. Bayesian regression -
   a. An 'uncertainty' is added to each observation to account for measurement uncertainties in irradiation temperature, fluence, and the measured property.
   b. By assuming that the errors are normally distributed, it is possible to calculate the likelihood that the data is described by a given set of model parameters using Bayes theorem and Monte-Carlo sampling.
   c. The output of the method is a distribution of model parameters, from which uncertainties can be calculated

The following sections of this appendix provide an example of parameter estimation and uncertainty assessment of dimensional (volume) change.

C.2 INPUT DATA

The ETU-10 graphite data for this statistical analysis are presented in Reference 59, compiled into a spreadsheet provided by ORNL "Ibiden_Technical_Details.xlsx". The provided data contain measurements of multiple graphite physical properties, but in this analysis only those in the 'Dimensional Comparison' worksheet are used. The data is also provided in tabular form in Table C-1.

C.3 DATA SCALING

Following best practices, the temperature and fluence values are normalized using a maximum scaler (so that the maximal absolute value of each feature in the data is 1.0). The dimensional change values are not normalized as this was not numerically required and the information regarding shrinkage and growth can be retained in the models.

C.4 ASSUMED UNCERTAINTY IN THE DATA

There is experimental uncertainty on the measurements of fluence, irradiation temperature and dimensional change. It is assumed in this analysis that the uncertainty on these parameters is as follows:

- Temperature, T, [°C]: [[

]]

- Neutron fluence, F, [x10^{25} n/m^2, E>0.1MeV]: An uncertainty of ±5% of the measured fluence;
- Dimensional change, ΔV/V0 , [%]: A set uncertainty of 1 μm for all length measurements. This is justified by ORNL's use of a 50 mm Mitutoyo micrometer of 1 μm accuracy (Reference 19).

C.5 MODELING APPROACHES

ORNL/TM-2017/737 (Reference 59) proposes trend lines for the evolution of dimensional change with fluence at various irradiation temperatures. In the ORNL analysis, each trend line is fitted to a group of data points for which the irradiation temperature is considered constant (the trend line model considers only fluence as independent variable, and not temperature). In addition, each trend line is fitted to a group of data points that have a common target irradiation temperature. This leads to nearly 200°C difference in measured irradiation temperatures among specimens fitted by the same 'temperature-independent' model, as shown in Figure C-1. The average measured temperature is reported by ORNL as the irradiation temperature for the group/trend line. The consequence of this approach is that the influence of as much as 200°C difference in irradiation temperature on dimensional change is not accounted for.

In contrast with the ORNL approach, the approach proposed by Kairos Power accounts for both irradiation temperature and fluence on dimensional change in regression models, which is motivated by the known influence of irradiation temperature on dimensional change. Kairos Power's approach also allows estimating uncertainties in parameters and in turnaround fluence. Only measurement uncertainties are captured here. Variability in irradiation data from variabilities in graphite (within-billet and billet-billet) is discussed in Appendix B.

C.5.1 ORDINARY LEAST-SQUARES (OLS) REGRESSION

OLS regression modelling is a method for estimating the unknown parameters in a linear model by minimizing the sum of the squares in the difference between the observed and predicted values of data. The analysis presented here was performed using the statsmodels package in Python (Reference 67).

OLS was used to select the model functional form initially down from several candidates. The approach taken was:

- To use only linear models - a linear model here is one in which the dependent variable is a linear combination of the independent variables including interaction terms (aka multiple linear regression with interactions)
- To use a model for which the dimensional change was zero (with uncertainty) at zero fluence.
- Find the best performing model whilst ensuring: i) The number of parameters is minimized; ii) The parameters in the model are all statistically significant. This was done via a combination of the Akaike Information Criterion (AIC) and the p-value of the parameters in the regression model.

The chosen model form used in the remainder of this analysis is:

$$\frac{\Delta L}{L} = \alpha + \beta_1 F + \beta_2 F^2 + \beta_3 FT$$

Where β is the set of unknown coefficients being solved for and α is an intercept parameter determined by the uncertainty on measuring zero dimensional change. The OLS regression model fitted to this functional form is referred to as the *baseline model* in the remainder of this technical note.

The 'bootstrapping' approach to determine the unknown parameters accounting for uncertainty in the fitted parameters and the measurement data is as follows:

1. For each measurement, sample from the uncertainty in the dependent and independent variables to create a new "pseudo" data point which represents a potential value, accounting for measurement uncertainty.
2. Fit an OLS model to this new "pseudo" dataset and intercept and find the optimized parameter covariance matrix.

This process is repeated for a large number, M, of random samples, resulting in a set of covariance matrices for the parameters. Each covariance matrix represents a possible set of parameters and the uncertainty for a pseudo dataset.

The uncertainty on the turnaround fluence F_{TA} is found by taking a large number, N, multivariate normal samples from each covariance matrix. Each sample gives a unique parameter set, β_{mn}, at which the turnaround fluence can be calculated as a function of temperature. This is done analytically by taking the differential of the equation for the baseline model:

$$F_{TA_{mn}} = \frac{-\,(\beta_{1_{mn}} + \beta_{3_{mn}}T)}{2\,\beta_{2_{mn}}}$$

The result is a distribution of F_{TA} at each irradiation temperature which can be used to calculate the best-estimate and uncertainty. In this analysis M=1000 and N=1000 which is sufficient to adequately define the distributions at a 95% confidence level.

C.5.2 BAYESIAN REGRESSION:

In Bayesian regression modelling, the variables are not treated as point estimates, as in OLS, but are formulated instead as uncertain inputs with a defined probability distribution. The analysis presented here was performed using the PyMC3 package in Python (Reference 68).

For a Bayesian model, priors must be assigned to the unknown variables in the model. For this linear regression model the priors are normally distributed. In this analysis, the priors were assigned as follows:

- The priors for the unknown coefficients in the equation for the baseline model (β_1, β_2, β_3) are normal distributions with mean and standard deviations as calculated by the OLS fit. It is recognized that these are a highly informed prior distributions, but this is judged appropriate given the information gained from OLS regression is a good description of the underlying data. The temperature and fluence priors are the centered at the measured value with standard deviation of the measurement uncertainties, as defined above.
- The uncertainty in $\Delta V/V_0$ measurements is included as a normal prior, with standard deviation of the estimated measurement uncertainty.

- The Bayesian model predicts outcomes $\Delta V/V_0$ as normally distributed observations with observation error s, with a half-normal distribution as the prior.

The No-U-Turn Sampler (NUTS) was used as it takes advantage of gradient information from the likelihood to achieve much faster convergence than traditional sampling methods. NUTS also has several self-tuning strategies for adaptively setting the tuneable parameters of a Hamiltonian Monte Carlo sampler. A total of 2,000 Monte-Carlo samples were used per chain.

The uncertainty on the turnaround fluence F_{TA} is found by taking each of the Monte Carlo samples for the unknown coefficients and analytically calculating the F_{TA} at each irradiation temperature using the equation above for F_{TA}.

C.6 RESULTS

See Table C-2.

Also, Figure C-2 illustrates the results from an OLS regression and a Bayesian regression.

Table C-1. Summary of ORNL Data for ETU-10 Dimensional Change

[[

]]

[[

]]

[[

]]

[[

]]

[[

]]

[[

]]

[[

]]

[[

]]

[[

]]

[[

]]

Table C-2. Results from OLS and Bayesian Modeling

[[

]]

Figure C-1. ORNL Report Grouping of Data by Target Temperature Compared to Measured Irradiation Temperatures.

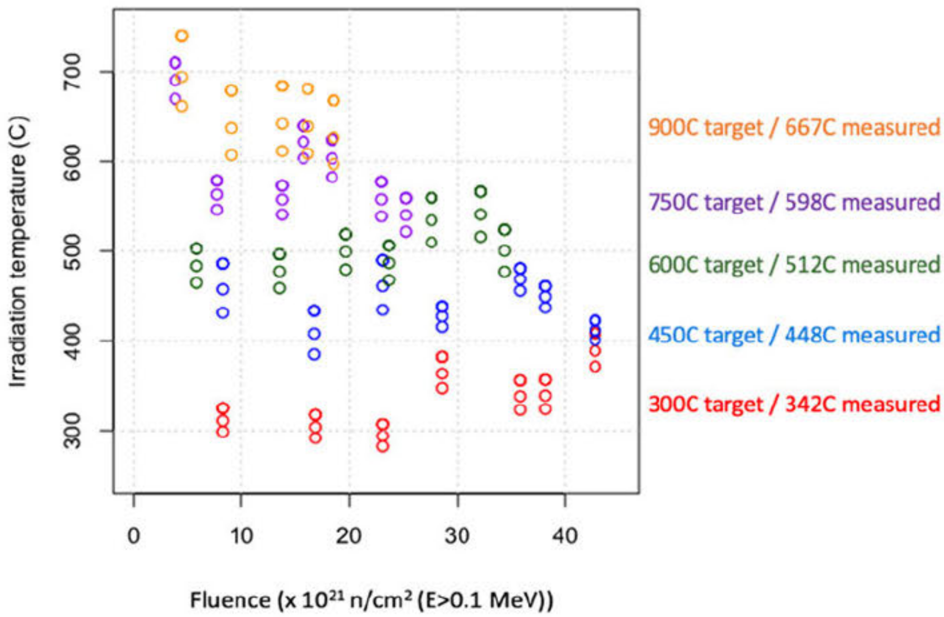

ORNL regression modeling (i.e., trend lines in the ORNL report ORNL/TM-2017/737) is performed on each group and does not account for the large temperature difference within a group and the overlap between groups.

Figure C-2. Turnaround Fluence as a Function of Irradiation Temperature for the Volumetric Dataset Using the OLS (left) and Bayesian (right) Regression Methods.

[[

]]

APPENDIX D. Comparison of IG-110 and ETU-10 Material Properties

Both ETU-10 and IG-110 are iso-statically molded superfine graphite with similar grain size. Their typical property values from manufacturers are listed in Table 15. ETU-10 has slightly lower density, but higher strength. The value of the Young's modulus is similar for both materials. Also for both materials, the fracture toughness value is in the range of typical superfine graphite (References 55 and 56).

Table 17 presents data from ORNL comparing the IG-110 and ETU-10 properties measured from one section of an individual billet. The deviation of data reported by manufacturer and ORNL is mainly due to the specimen size effect and number of samples tested as well as the test method. The comparison of ORNL data was made for those specimens with similar dimension to minimize the specimen size effect. The data show that the properties of the two materials are similar. ETU-10 has lower CTE, but higher anisotropy ratio than IG-110. ETU-10's anisotropy ratio classifies it as a near-isotropic graphite (but at borderline), while IG-110 is isotropic. Thermal conductivity of ETU-10 is lower than IG-110 at room temperature, but they are equivalent at 500°C.

The graphite pore structure affects not only its mechanical property response to the irradiation, but also affects molten salt infiltration. The pore structure of ETU-10 and IG-110 is compared in Table 18. Both materials have similar pore structure with ETU-10 having slightly higher open porosity. ETU-10 shows higher mercury (Hg) intrusion volume, which implies ETU-10 may be infiltrated with more salt in the event of full infiltration, compared to IG-110. The entrance pore diameter is a key parameter in determining the molten salt infiltration threshold pressure. The value for the two materials is very close for the test specimens.